Contract n° ***MAS3-CT97-0090 (DG 12 - ESCY)***

Title

CHARACTERIZATION AND OBSERVATION OF THE SEAFLOOR WITH A NEW MULTI-BEAM FRONT-SCAN SONAR SYSTEM

Acronym

COSMOS

Final report on Task 2

Hardware Development

including

Task 2.1 *: Antennae*

Task 2.2 *: Electronics at Transmit and at Receive*

Task 2.3 *: Data Links and Storage, System Controls and Displays*

UNIVERSITÉ PIERRE ET MARIE CURIE
LABORATOIRE DE MÉCANIQUE PHYSIQUE
(CNRS UPRESA 7068)

Redactor : Pierre Cervenka

CONTENT

INTRODUCTION

The technical annex of the contract referenced the following reports with regard to Task 2 (Hardware development) :

- R2.1 Antennae and electronics (Tasks 2.1 and 2.2)
- R2.3.1 File formats for recorded data (Task 2.3)
- R2.3.2 Interfaces (Task 2.3)

The present text merges the three planed reports, in describing the deliverables of Task 2 that were all successfully achieved.

- Section 1 addresses Task 2.1 (antennae) with 2 deliverables :
  - Transmitter
  - Interferometric receiver
- Section 2 addresses Task 2.2 (Electronics) with 2 deliverables :
  - Transmitter
  - Receiver
- Section 3 addresses Task 2.3 (Data Links, Storage, System Controls and Displays) with 3 deliverables :
  - File formats for recorded data
  - HW and SW for data links and storage
  - HW and SW for system controls and displays

Concerning Task 2.3, an additional report from TEISA is appended. It describes the architecture developed by TEISA to collect and to store acoustical data, and to control the sonar system. This solution was not ready for the sea trials with the prototype system, but would be a more likely setup in the frame of an industrial product. The present report describes the setup which was actually used during the survey.

1. ANTENNAE

1.1 DESCRIPTION OF THE ANTENNAE

1.1.1 Objectives

This task concerns the design, building and testing of the antennae of the COSMOS prototype system. These antennae comply with the following requirements :

- The central frequency is 100 kHz.
- The aperture in site is similar to the vertical aperture of a sidescan sonar system (SSS), i.e. the insonified sector extends roughly from nadir to more than 75° incidence angle.
- The aperture in azimuth equals 25°. It covers the along-track band that is blind with SSS.
- The source level of the transmitter must be such that the slant range reaches a few hundred meters. The large solid angle to be insonified constitutes a limiting factor.
- The receiving antennae enable beam steering over the whole azimuth aperture. With about 32 formed beams, the – 3 dB beamwidth is around 1.5°.
- In addition, the receiving antennae provide the interferometric capability (bathymetry function).

1.1.2 Achievements

The first sea trial (Toulon, end of July 1999) failed because a small amount of water leaked in the electronics that is embedded in the receiving arrays. The conception of the antennae allowed to reach and to replace the damaged parts. The metal inserts from where originated the leakage were modified, and the whole problem was fixed in September. The performance of the final antennae experienced no discrepancy during the second survey (Barcelona, 22 October – 3 November 1999). The arrays were calibrated a first time, in January 1999, at the IFREMER's facility (large tank) - Brest. However, because of the repair performed in September, part of the calibration had to be done again in the LMP's tank (November 1999).

Two transmitting antennae have been built. The first antenna is shaped as kind of a torus in order to maximize the active surf ace. However, the 3-D field obtained with this antenna was not satisfactory (Test in IFREMER's tank). Hence, another transmitter had to be designed and built before the sea trials. Its shape is a simpler arc of a circle. This new version yielded satisfactory results (test performed in June 1999, at the IFREMER's facility, and operational behavior during the sea trials).

The technology of the transmitting and receiving antennae is based on composite 3-1 resin / PZT ceramics. The characteristics of the antennae are summarized in the following :

Receiver : two parallel rows of linear arrays

- Interferometric baseline = 2.5 wavelength
  (i.e. the spacing between arrays is around 4 cm)
- Length : 72 cm
- 32 elementary transducers per array
- Pitch : 22.5 mm.
- The active face of both arrays is looking forward, 40° below the horizontal.

Torus shaped transmitter

- 80 slice-elements arranged along an arc whose axis is vertical
- Average radius ≈ 1.5 m
- Inner curvilinear length ≈ 80 cm
- Emitting surface > 10 dm^2
- 16 piezoelectric rod per slice (Thickness = 10 mm).

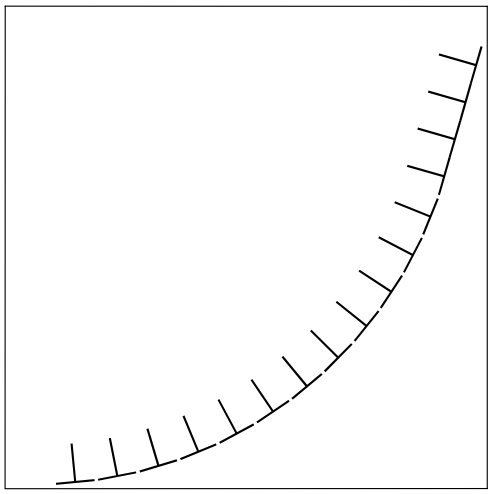

Figure 1.1 : Cross-section of a slice generating the torus shaped transmitter
(not to scale)

Transmitter shaped as an arc of a circle

- Radius ≈ 1.4 m
- Length of the arc ≈ 80 cm
- 125 active piezoelectric rods
- The antenna is slanted 40° below the horizontal,
  i.e. with the same angle as the receiving arrays.

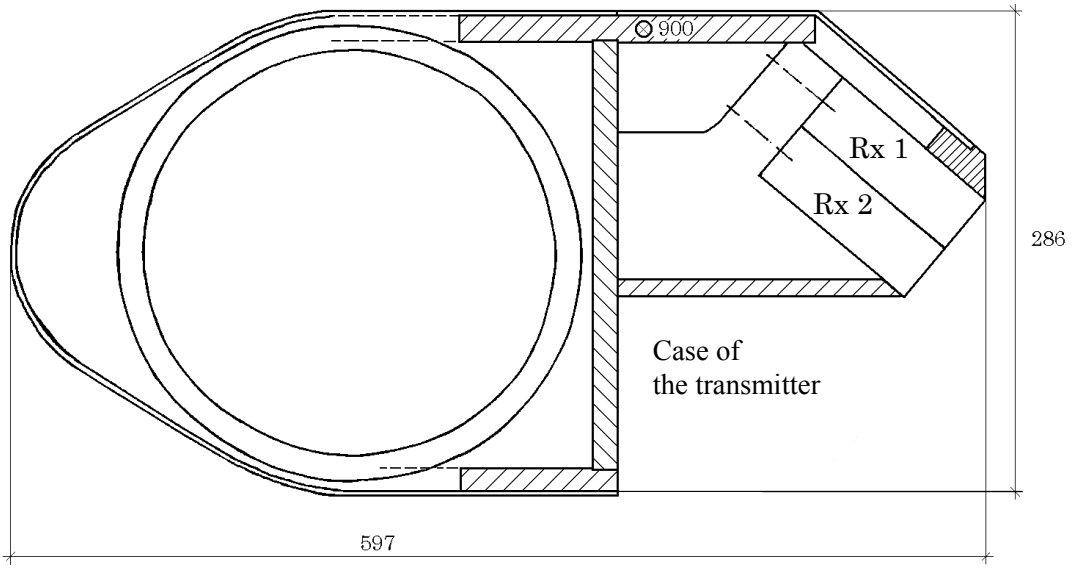

Figure 1.2 : Partial cross section of the downside unit.

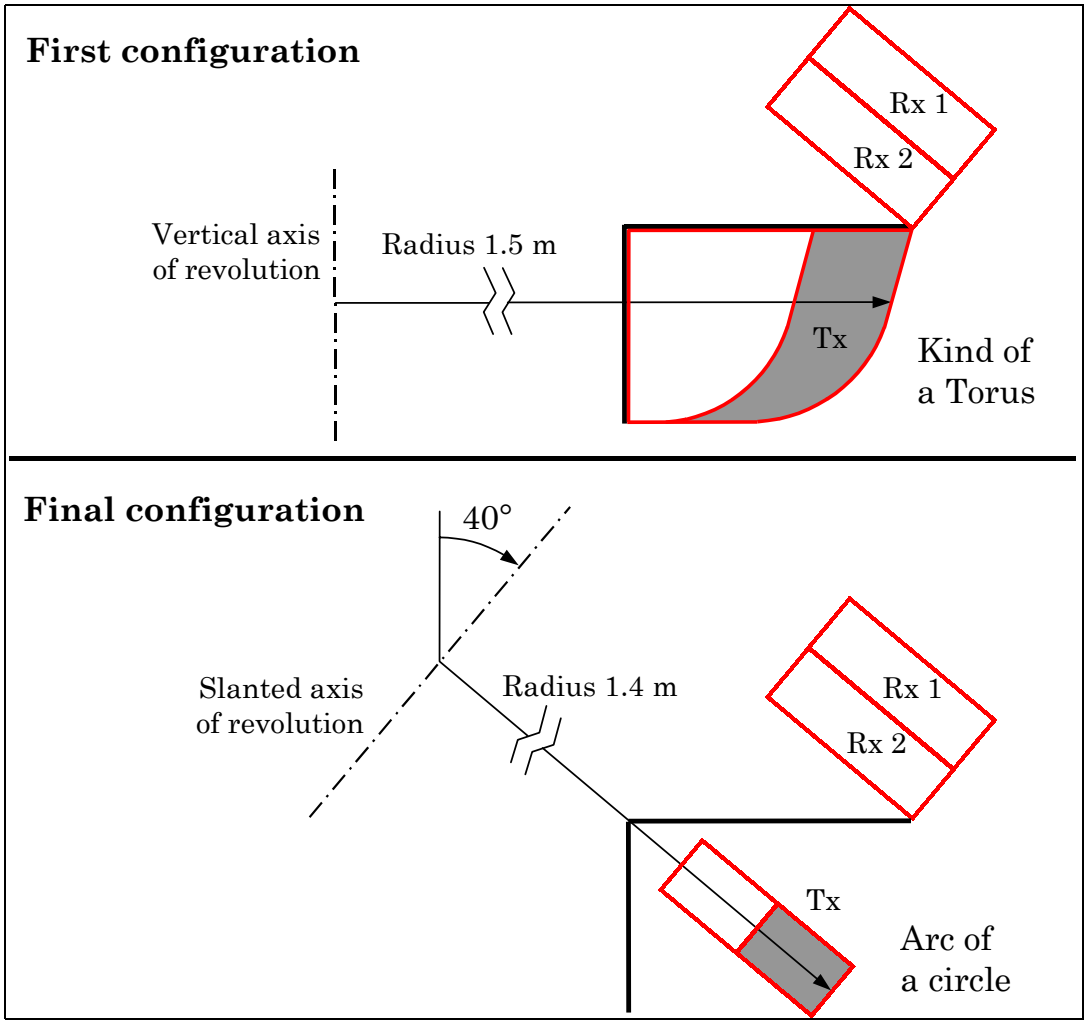

Figure 1.3 : Schematic side view of the antennae
(the active face of the transmitter is shaded)

The downside unit consists of both the transmitting antenna and the pair of linear receiving arrays, plus a cylindrical container located behind the antennae. This container accomodates part of the electronics. Figure 1.2 is a sketch of the cross section of the unit. Figure 1.3 shows the relative locations of the antennae in the unit. Figure 1.4 is a picture of the skeleton, laid on the nose.

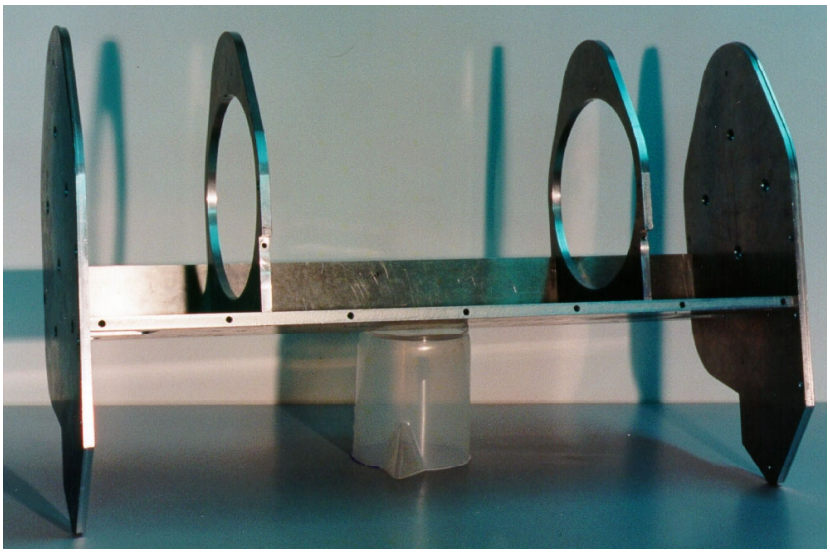

Figure 1.4 : Skeleton of the downside unit

But for the front part, the whole module is encased in a careen in order to reduce the drag effort. Most parts are made of anodized alloy. The complete module weights (dry) around 80 kg. The apparent weight in water is reduced to about 50 kg, the inertial mass being 100 kg because of the water trapped in the careen.

Figure 1.5 shows the frame that holds the antennae (turned upside down). An element of the torus shaped transmitter is in place. All elements are set in place in the rear view displayed in Figure 1.6. Figure 1.7 shows the front view of the torus shaped transmitter, still turned upside down, before final molding. A receiving array which has not received all its front end electronics is also displayed on the picture.

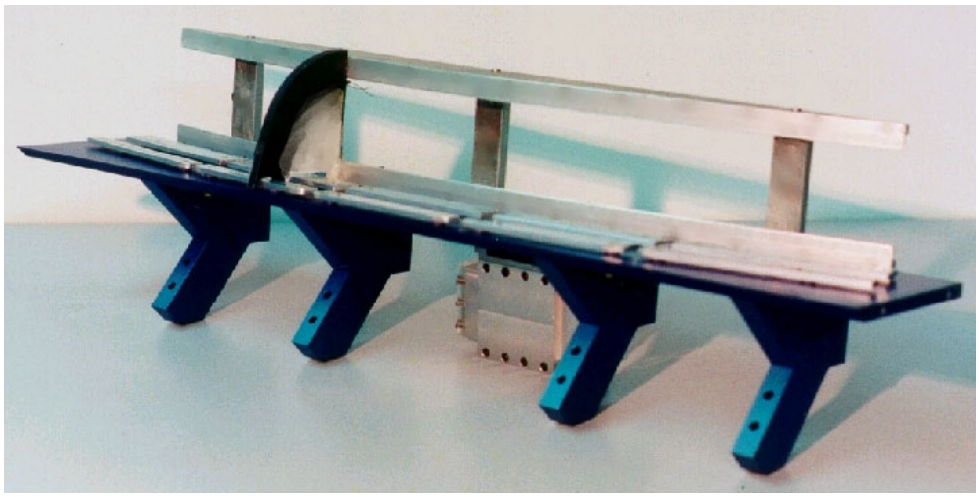

Figure 1.5 : Frame holding the receiving arrays and the torus transmitter (shown upside down)

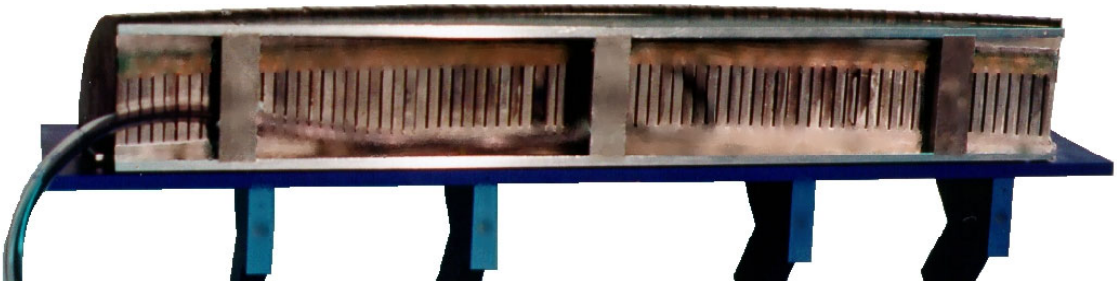

Figure 1.6 : Torus shaped transmitter (before final molding)
Rear view of the elements

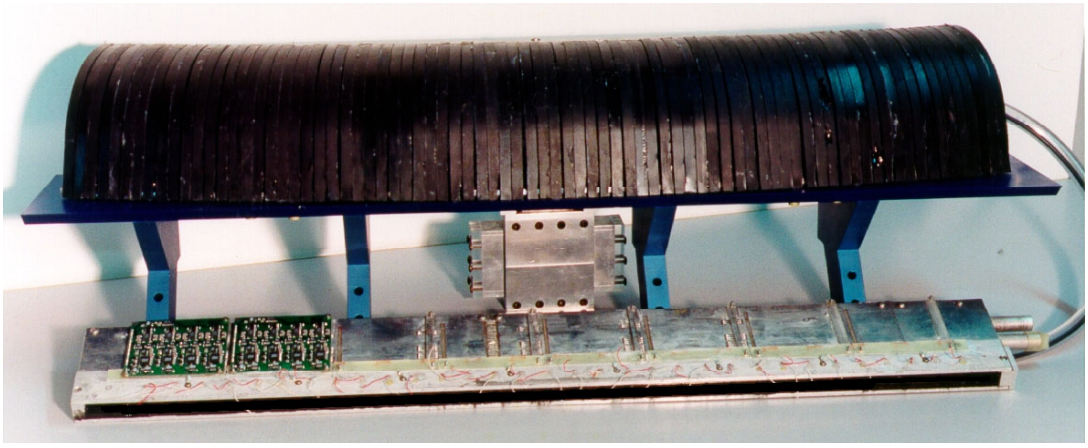

Figure 1.7 : Torus shaped transmitter (before final molding)
and part of a receiving array

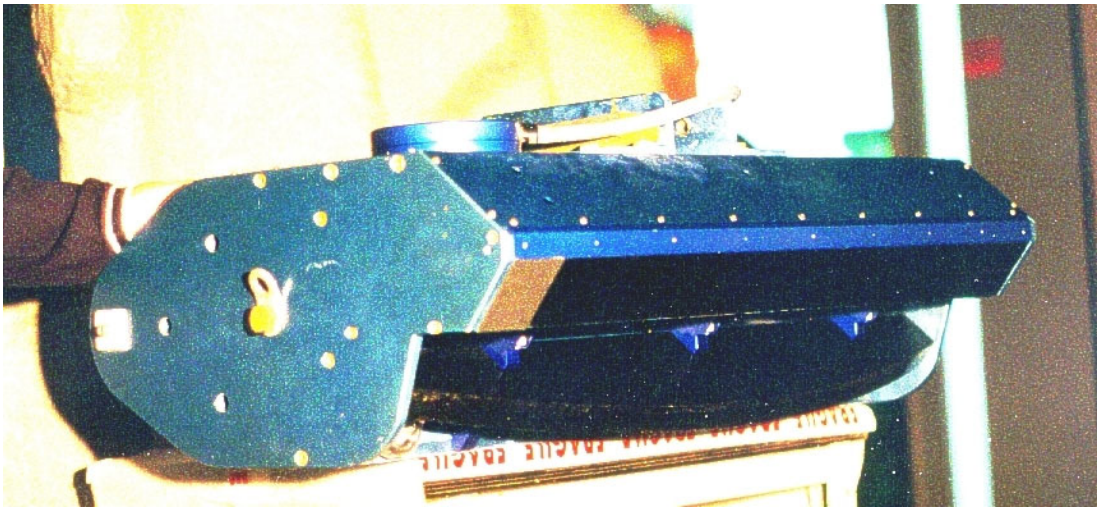

Figure 1.8 : Complete module, with the transmitter shaped as an arc of a circle

1.2 NUMERICAL TOOLS

Part of Task 2.1 consisted of the design of the antennae. Within the COSMOS project, several numerical tools have been improved or developed. They are briefly described in this section.

1.2.1 Echographic responses with two different antennae (2-D model)

A 2-D model allows to simulate the harmonic response of curvilinear arrays, computed at any distance, and to study the effect of many parameters, e.g. :

- Shape of the arrays, with non constant radii of curvature.
- Number and spatial repartition of the elementary transducers.
  Non constant pitches can be used to shade transmitting arrays.
- Orientation of the elements (not necessarily the same for all elements)
- Elementary directivities.
  Inputs can be measured values, or theoretical patterns.
- Amplitude and phase modulations of each element.
  It allows to simulate taper windows, focusing and beam steering,
  and to test the effect of inhomogeneous responses of the elements
- Relative location and orientation of the transmitter and of the receiver
  (for echographic responses)
- Effect of the digitization in the beamforming process.
- Search for the center of phase of antennae.
  Such an information is critical in the synthetic aperture technique.

1.2.2 Search for the radius of an arc of a circle (2-D model)

The geometric angular aperture of an antenna shaped as an arc of a circle is defined as the *curvilinear length of the arc* to *radius* ratio. Depending on the configuration, this angle can be significantly different than the resulting aperture of the acoustical field. This program takes as inputs :

- The imposed length of the arc
- The required angular aperture of the beam pattern

The output is an estimate of the optimal radius of the antenna.

1.2.3 Profile optimization (2-D model)

During the COSMOS project, a specific program has been written in order to define the optimal cross section of the torus shaped antenna, together with the orientation of the receiving array. The beam pattern obtained with this antenna was jeopardized because the torus has been generated with a vertical axis of revolution, instead of taking a slanted axis. However, the modeling of the cross section itself is correct.

Given several weighted constraints, the optimization process seeks to minimize a cost function that is derived from the echographic diagrams obtained by scanning a

space of parameters (curvatures, orientations, …). Three main factors are taken into account with respect to the diagram in the alongtrack vertical plane :

- The maximal level of the echographic response and its direction :
  The maximal level must be sent to the direction where losses are the largest, i.e. at the maximal slant range. The project targets at a scanned sector that is roughly 75° wide in site, so that this direction is around 15° below the horizontal.
- Another concern is the relative level of the parasitic echoes that may be received from the horizontal direction and upward. These interferences are originated either from direct backscattering by the sea surface, or from multiple travels between the seafloor and the sea surface.
- The size of the blind sector in the near nadir area :
  The gradient of the echographic response in site of the antennae, close to the vertical direction, dictates the extent of this sector (diaphony with echoes received simultaneously from behind the across-track vertical plane).

1.2.4 Echographic responses with two different antennae (3-D model)

We built a complete 3-D modeling tool in order to analyze the problem encountered with the first transmitter, and to check the design of the new version. This software enables to compute the echographic field of a pair of antennae. The shape of the transmitter can be complex, but the receiver is necessarily a linear array. The orientation of the antennae can be adjusted at will. Several types of representation are available :

- Projection on a flat bottom
- Constant beam steering angle (fixed distance, variable is site plane angle)
- Constant site plane (fixed distance, variable is beam steering angle)
- Constant azimuth plane (fixed distance, variable is grazing angle).
- Constant grazing angle (fixed distance, variable is azimuth plane angle)

1.3 RECEIVING LINEAR ARRAYS (measurements)

Each linear array that constitutes the receiving antennae is built with a single row of piezoelectric components. A short prototype module, made of 16 piezoelectric components, has been tested to estimate the response in site. The measurements have been processed to produce a symmetrical pattern (Figure 1.9) before being inserted in numerical models.

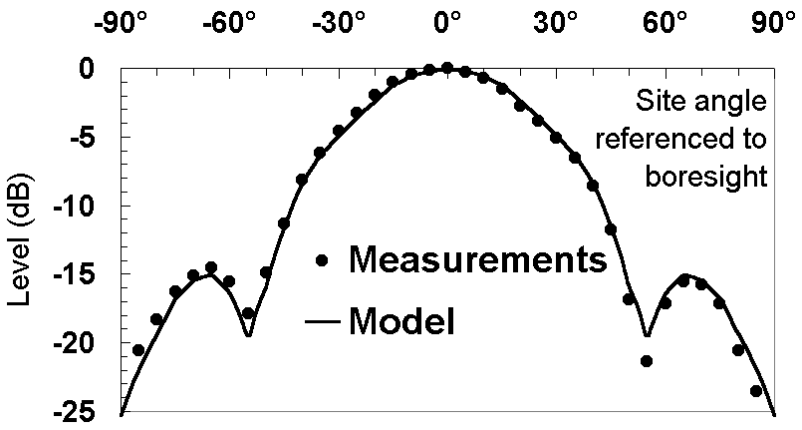

Figure 1.9 : Preliminary model for the response in site of the receiving arrays

The complete arrays have been tested at the IFREMER's facility (25-28 January 1999). The aim of the experiment was to measure the global sensitivity of the arrays, and to check that :

- the aperture in site is smooth and large enough to cover the required aperture ;
- the angular acceptance in azimuth of the elementary transducers is sufficient with regards to the 25° wide sector to be scanned.
- the interferometric response is single-valued (but for the 2π ambiguity) over the whole range of site angles

1.3.1 Site

In order to measure the response in site (null azimuth) of the arrays, and to calibrate the interferometer, the system is tilted at a right angle compared to the normal operating geometry (Figure 1.10) : The COSMOS module is hung vertically by its side, at a depth of 5.3 m (center of the module). A small probe is located at the same depth, at an horizontal distance of 25.3 m. Both the probe and the wet module are aligned in the median vertical plane of the tank. The module is rotated by 1° around the vertical axis between each measurement.

The probes transmits a Linearly Frequency Modulated signal (Chirp : Central Frequency 100 kHz ; Bandwidth 3 kHz ; Duration 3 ms). The signals received by each elementary transducer of the arrays are recorded by the COSMOS system.

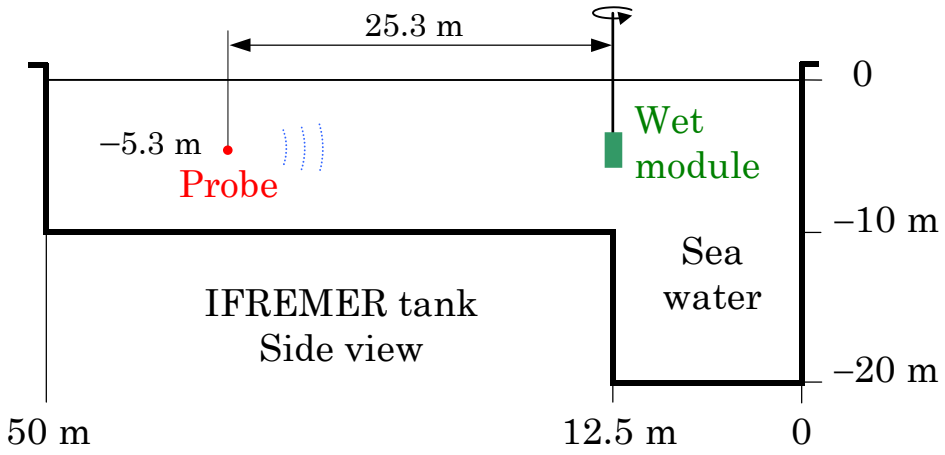

Figure 1.10 : Configuration #1 at the IFREMER's tank.
COSMOS module hung by one side

At a post-processing stage, the records are pulse compressed. The time sample that holds the maximal magnitude is searched. The phases of the selected values are unfolded. A polynomial regression (2nd order) allows to derive the direction and curvature of the wave front, hence providing an accurate relative location of the probe with respect to the arrays. According to these parameters, a beam is focused toward the so tracked target. The amplitude of the beamformed samples gives the operational response in site of the arrays. In addition, the conjugate products of the beam samples obtained with both arrays provide the interferometric relation between differential phases and geometric angles.

Figure 1.11 displays the diagrams obtained in site. The angles are scaled as in the normal operating geometry, i.e. 0° tags the horizontal direction and 90° points vertically downward. For both arrays, the width of the response in site (null azimuth) is found to be around 55–59° at –3 dB, and 81° at –6 dB. The latter aperture extends roughly from the surface to about 10° incidence, which complies with the requirements of the COSMOS system. This result is close to the preliminary experimental estimate (Figure 1.9) derived with the mini-array, i.e. 46° and 69°, at –3 dB and at –6 dB respectively.

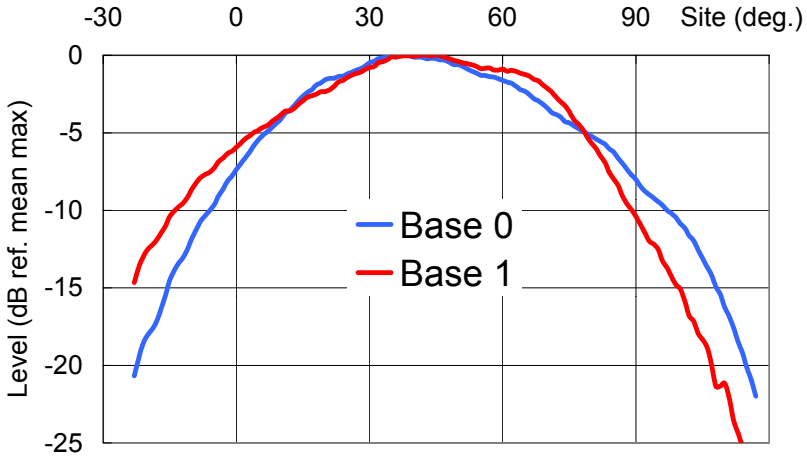

Figure 1.11 : Response in site of the receiving arrays
(Magnitude of beams formed toward source)

1.3.2 Azimuth

The next experiment was made with the wet module hung by its normal, upper attachment, but tilted 40° upward (Figure 1.12). Doing so, boresight of the receiving arrays scans the horizontal plane (that contains the transmitting probe) when rotating the module. The post-processing procedure is the same as to measure the response in site.

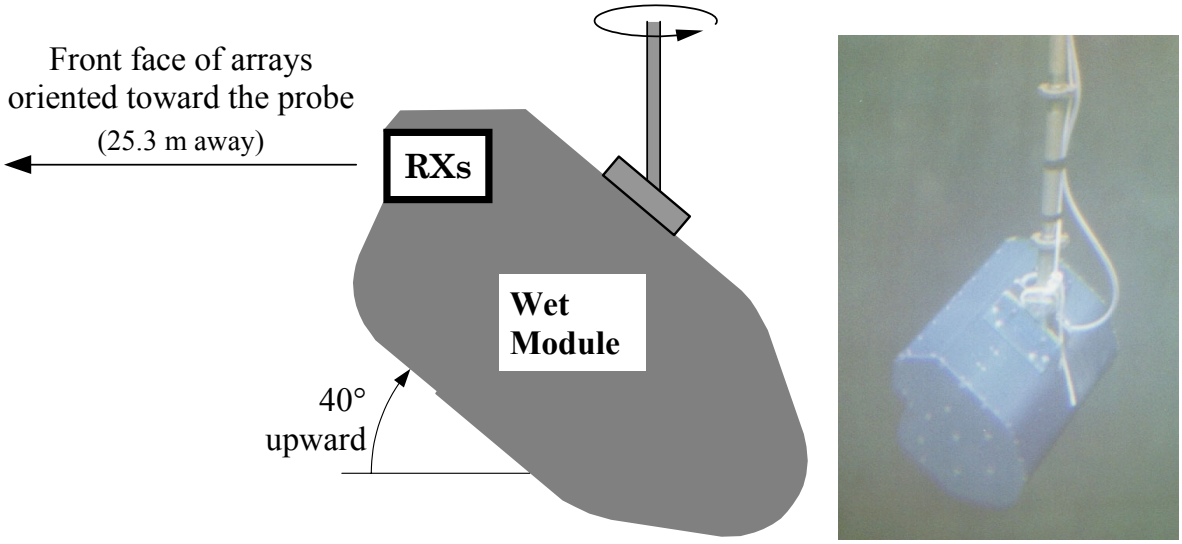

Figure 1.12 : Configuration #2 at the IFREMER's tank

The result (Figure 1.13) can be interpreted as an average response in azimuth of the elementary transducers that constitute the arrays. The angular acceptance is found to be around 45° and 33°, at –6 dB and at –3 dB respectively. Such an aperture is comfortable compared to the required 25°.

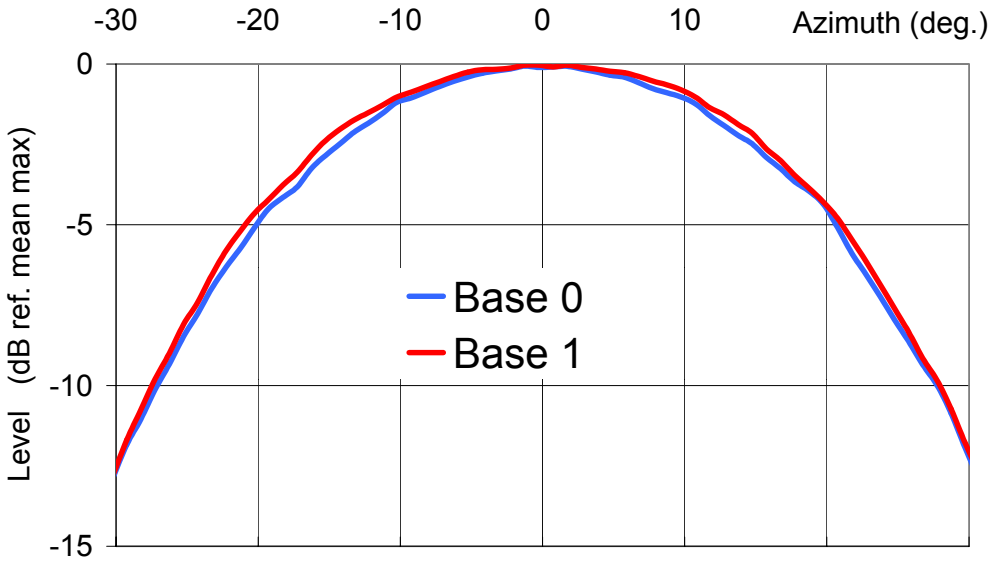

Figure 1.13 : Response in azimuth of the elementary transducers
(Magnitude of beams formed toward source)

The theoretical 2D diagram of a beam formed with the arrays is displayed Figure 1.14. Figure 1.21-c shows the field pattern of such a beam, computed within a 3D-model (projection on a 40 m deep flat ground ; The active face of the array is slanted 40° below the horizontal). The steering angle is 12.5° off-axis, using a Gaussian taper window (truncated at 20% at ends) in the beamforming process.

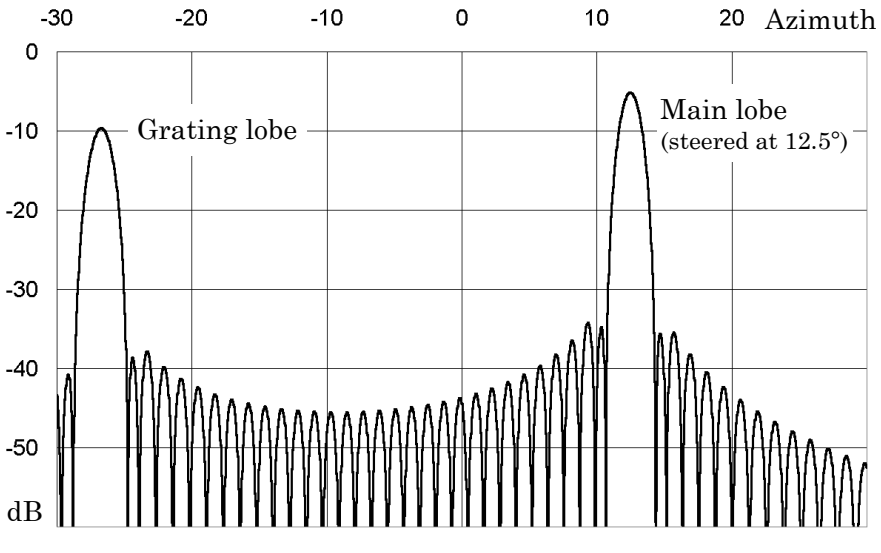

Figure 1.14 : Diagram in azimuth of the receiving array . 2-D model (steering at 12.5°)

The pitch of the arrays is 1 ½ wavelength (22.5 mm). This relatively large pitch eases the integration of the front-end electronic molded in the antennae, whereas the limited number of elements reduces the overall complexity of the system. The drawback is that grating lobes arise on the opposite side of the steering direction, as can be noticed in both Figures 1.14 and 1.21-c. However, the transmitter does not insonify the areas where these grating lobes take place, so freeing the echographic response of potential artefacts.

1.3.3 Interferometer

The interferometric lookup table that has been derived with the first configuration used in the IFREMER' tank is displayed Figure 1.15. Notice that the geometric angles are referenced to boresight. Within a theoretical model that assumes point-like receivers, the dependency of the differential phase, φ, with the geometric angle, θ, is given by $\varphi = 2\pi D \sin\theta$, where D is the interferometric baseline counted in wavelength. The measurements match closely this model by taking D = 2.13. The actual interferometric baseline is slightly larger. The discrepancy with the theoretical model is caused by the finite width of the arrays. Anyhow, the important conclusion is that the phase/geometric angles relation is single valued. The presented calibration is only meant to initialize the look-up table that is used in the process that derive the bathymetric samples. The objective of the self-calibration procedure that is included in Task 4.2 is precisely to refine and to update this look-up table, by taking into account the actual conditions of the data collection (that depends for example of the temperature close to the antenna, and of the current bathy-celerimetry profile).

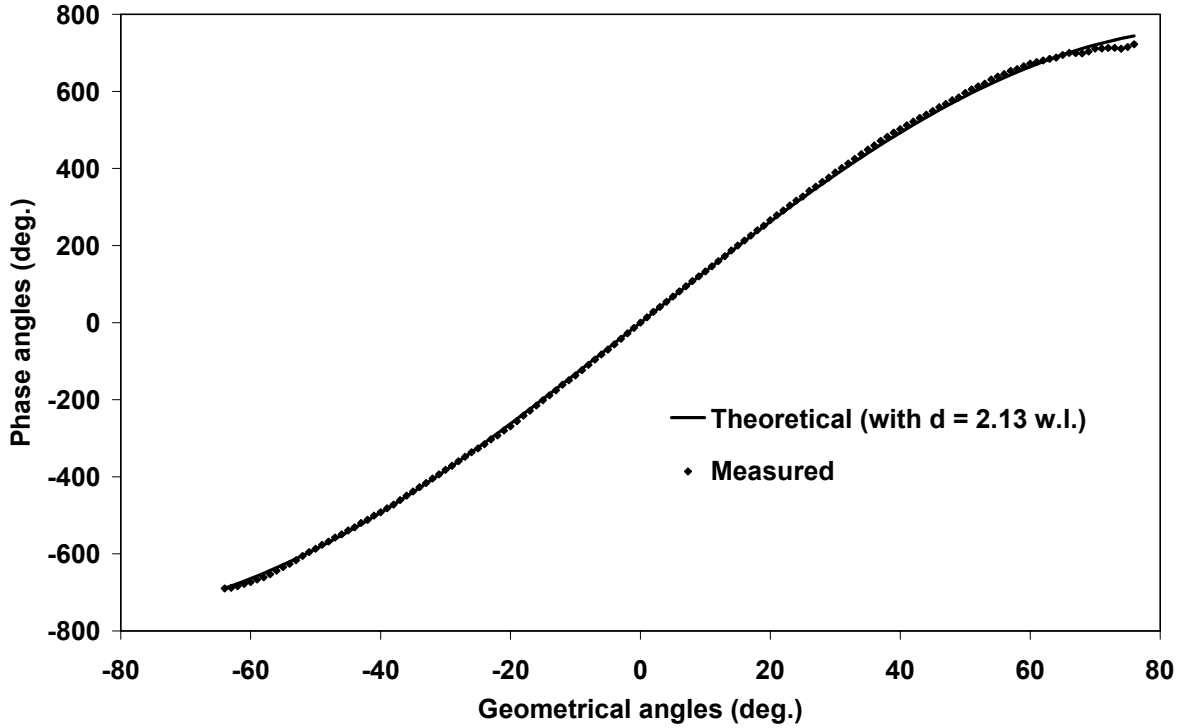

Figure 1.15 : Interferometric calibration

1.3.4 Sensitivity

In both experimental configurations, a calibrated hydrophone was located close to the COSMOS module in order to measure the incoming acoustic level. It allowed to derive the sensitivity of the receiving arrays. For this measurement, the probe transmits short pulse (300 µs) at a constant frequency (100 kHz). The obtained sensitivity is the same for both arrays, and is expressed here in terms of numerical unit, as recorded, per unit of pressure :

SH = –91.5 dB (ref. 1 bit / µPa)

1.3.5 Elementary transducers calibration

The electronics delivers in-line beamformed data. However, this process does not take into account any compensation for the individual variations between the transducers responses. During the sea trials, a very large amount of data have been collected. So, it has been decided to re-compute the beams, at a post-processing level, from the recorded complex data corresponding to the signals received by each transducer. Therefore, the relative response (sensitivity and phase) of each transducer has been calibrated as follow :

The energy of the signals recorded during the whole survey is averaged for each transducer. It has been checked that the electronics does not introduce any unbalance between the real and imaginary parts. Figure 1.16 displays the results in terms of amplitudes. This table allows to compensate for the uneven sensitivity of the elements, hence reducing the level of the side-lobes that are inherent to any beamforming process.

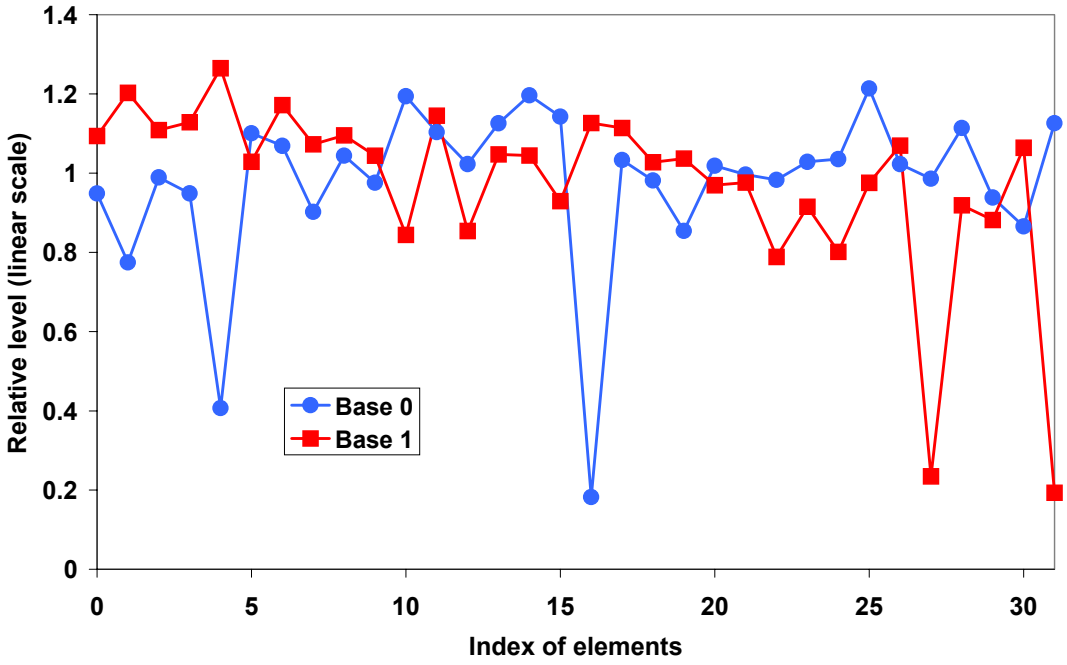

Figure 1.16 : Sensitivity of each elementary receiving transducer

There is no way to derive the phase dispersion of the elements from such statistics as for the amplitude sensitivity. Hence, an experiment that is very similar to the one performed at the IFREMER's facility has been done at the LMP's tank (Figure 1.17).

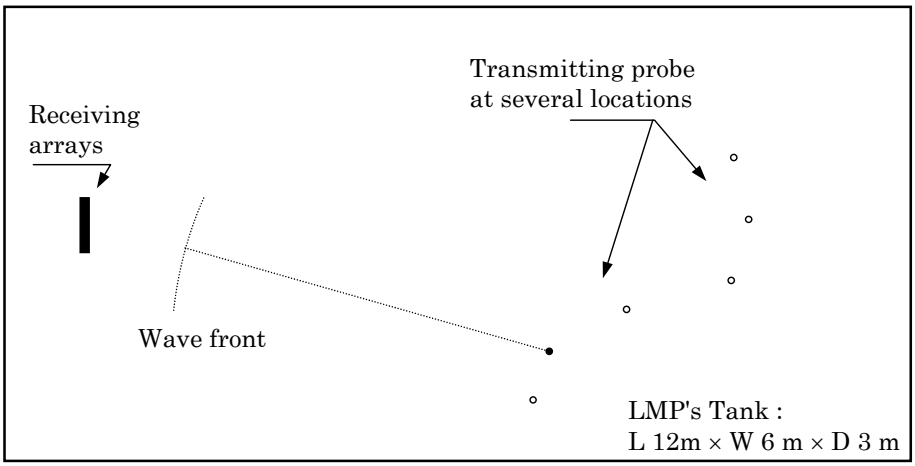

Figure 1.17 : Experimental setup for calibration in phase of the receiving arrays

Given a location of the transmitting probe, the phases of the pulse compressed signals undergo a least square fitting with a parabola. The differences are recorded. The process is iterated using different locations of the probe, in order to check that these differences are consistent (i.e. given a transducer, the variance in the differences between the recorded phases and the parabolae is small). Hence, the averaged values (Figure 1.18) yield reliable relative phase offsets that can be compensated for, together with the amplitude correction. To this respect, it can be noticed that the behavior of a few elements departs significantly from the average response (weaker sensitivity and relatively large phase offset). However, the consistency of

the phases obtained in the experiment depicted Figure 1.17 showed that these elements are functional and must be taken into account.

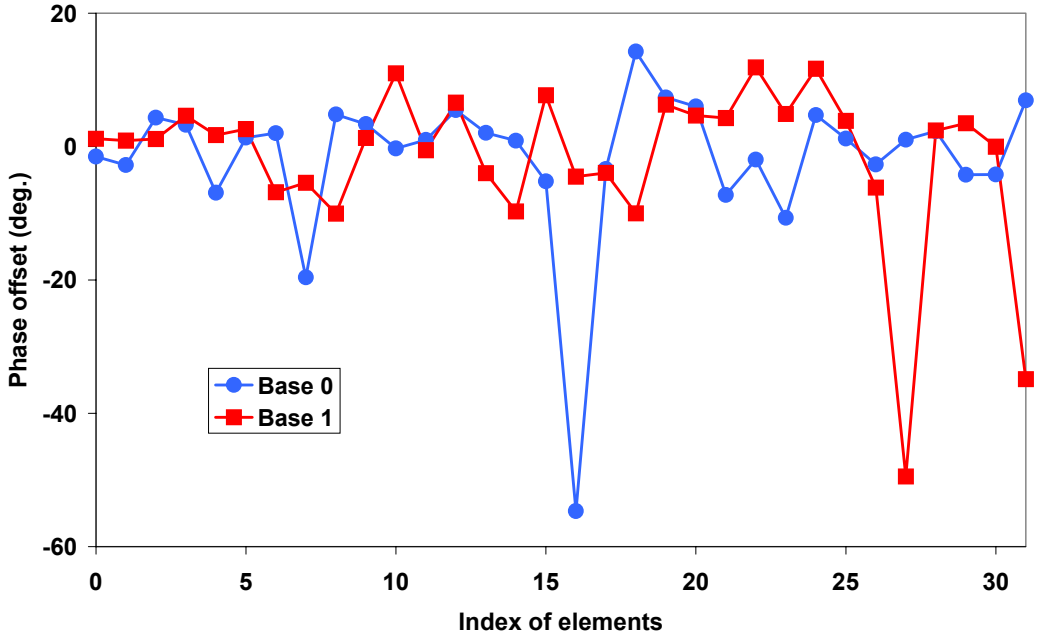

Figure 1.18 : Calibration in phase of each elementary receiving transducer

Note that the global sensitivity of the arrays have been checked again, i.e. after the survey in the LMP tank. We found no significant difference with the SH figure derived in the IFREMER's tank, i.e. before the repair.

1.4 TRANSMITTERS (models and measurements)

1.4.1 Torus

Figure 1.19 displays the 2-D theoretical response in site of the cross-section of the torus transmitter (Figure 1.1), combined with the diagram used to model the linear arrays (Figure 1.9, assuming boresight is oriented 40° below the horizontal). The theoretical echographic response complies with the requirements asserted in the optimization process that is described in Section 1.2.3.

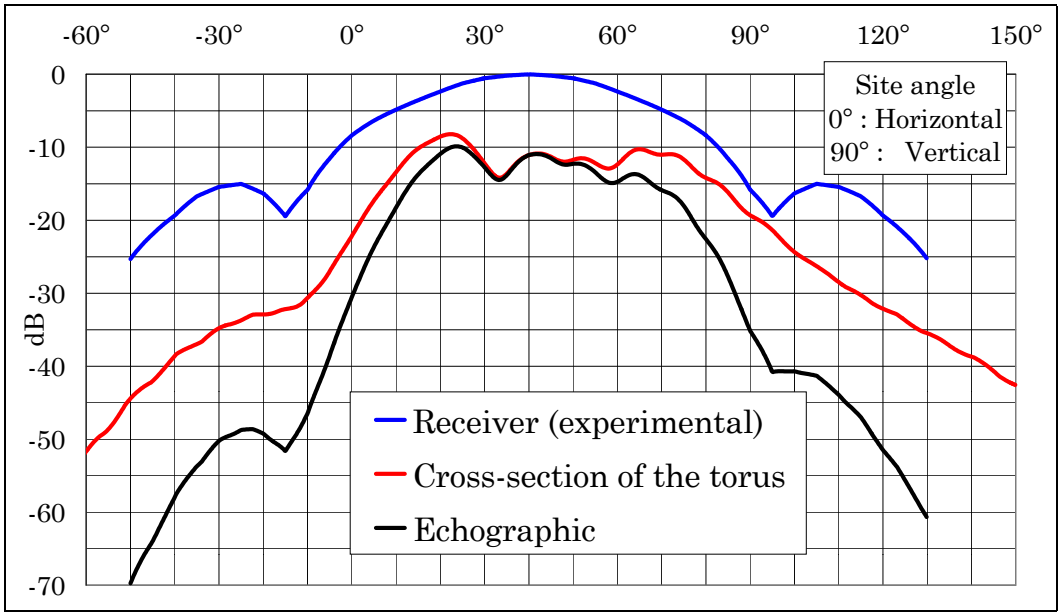

Figure 1.19 : 2-D model for the response in site

The actual diagram in site (Figure 1.20) of the torus shaped transmitter has been recorded in the IFREMER's tank, using the configuration #1 depicted Figure 1.10. This configuration corresponds to a null azimuth in the operational geometry, with varying site angles.

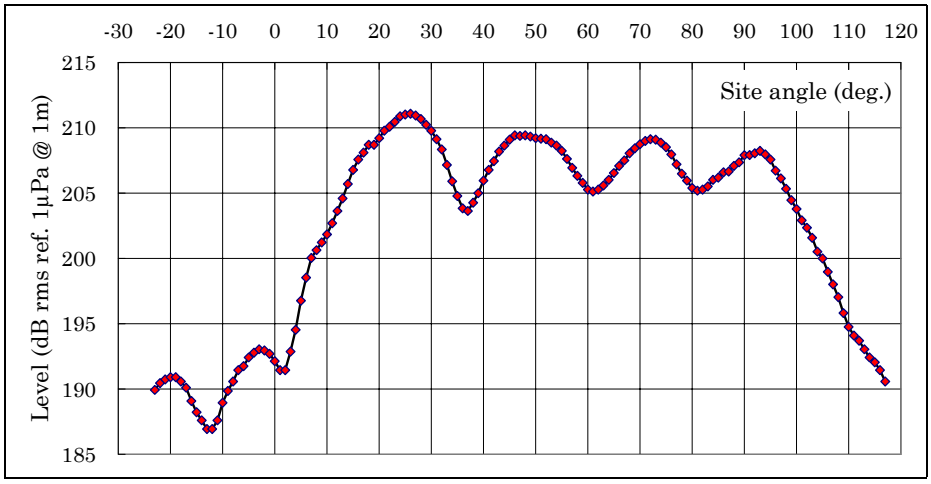

Figure 1.20 : Diagram in site of the torus shaped transmitter

The sharp roll-off that can be observed before 15° is excellent to reduce the amount of energy sent toward the surface (0°) and above. However, the level that is sent to what corresponds to the nadir area in operational conditions (site around 90°) is much higher than expected.

The cause is that the directivity of the antenna is very sharp in the direction of its axis of revolution, a phenomenon that the 2-D model does not put in evidence. This effect is clearly seen in Figure 1.21-a, where the theoretical field of the torus is computed with a 3-D model on a flat bottom (depth 40 m). However, the poor rejection of echoes that come from behind the vertical across-track plane with respect to those that come from the front area is not the worst drawback.

The most detrimental consequence of the high directivity in azimuth appears by looking at the directivity pattern of the receiving arrays, when the beam is steered off axis (12.5° in Figure 1.21-c). For small to medium incidence angles, the arrays focus on an area than is not properly insonified by the transmitter. As a result, echoes that originated from the grating lobe direction are not properly rejected in the echographic response, as shown in the left part of Figure 1.22 (zooms on the nadir area). In addition, the sidelobes of the receiving arrays are emphasized, as they fall plainly in the highly focused transmitted beam pattern.

The above mentioned problem is significant for the incidence angles up to more than 30°. This reason is sufficient to disqualify this transmitter for the sea trial. It must be noted that the same cross-section could have been used to shape another efficient transmitter, but using a slanted axis of revolution. However, the size of such an antenna would be much more cumbersome, and would not fit in the existing frame of the wet module. Hence, it has decided to build another transmitter, shaped as a simple arc of a circle.

1.4.2 Arc of a circle

Figure 1.21-b shows the expected field of the transmitter built according to an arc of a circle, the revolution axis being slanted by 40° from the vertical. With this new geometry, the insonified sector in the nadir area is much larger than with the torus whose axis is vertical. The right part of Figure 1.22 shows that the grating lobes are properly rejected in the echographic response (< –30 dB). There is no significant rising of the sidelobes either. Figure 1.23 displays the echographic responses computed over the front area of interest, for several steering angles. Grating lobes remain always at an acceptable low level, thanks to the theoretical shape of the transmitted field. It is therefore mandatory to check that the actual beam pattern generated by the transmitter is correct.

Tests have been performed in the IFREMER's tank, in June 1999. Figure 1.24 displays the setup. The revolution axis of the arc of circle is slanted 40° with respect to the vertical. For a given set of measurement, the horizontal distance between the transmitter and the hydrophone is a constant. Diagrams at a constant grazing angle are obtained by rotating the transmitter around a vertical axis. The transmitter sends a short pulse (300 µs) at a constant frequency (100 kHz). Several experimental results are shown Figures 1.25, together with the 3-D simulation (nearfield computation, at constant grazing angles and ranges).

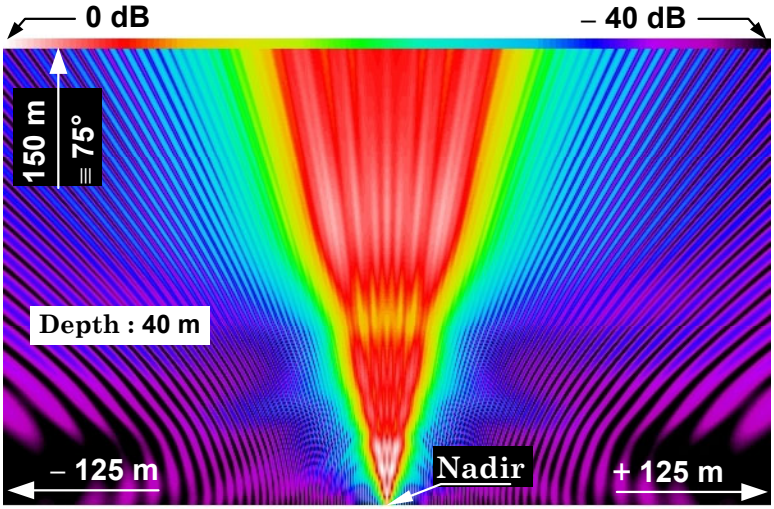

TORUS SHAPED TRANSMITTER (a)

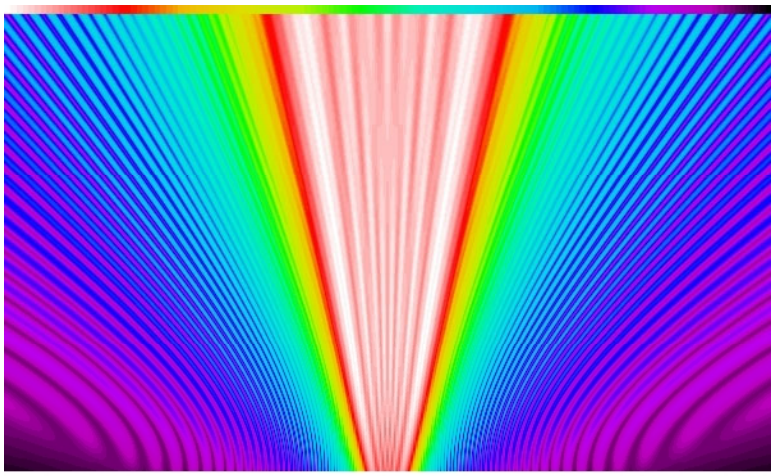

ARC OF A CIRCLE (axis slant : 40°) (b)

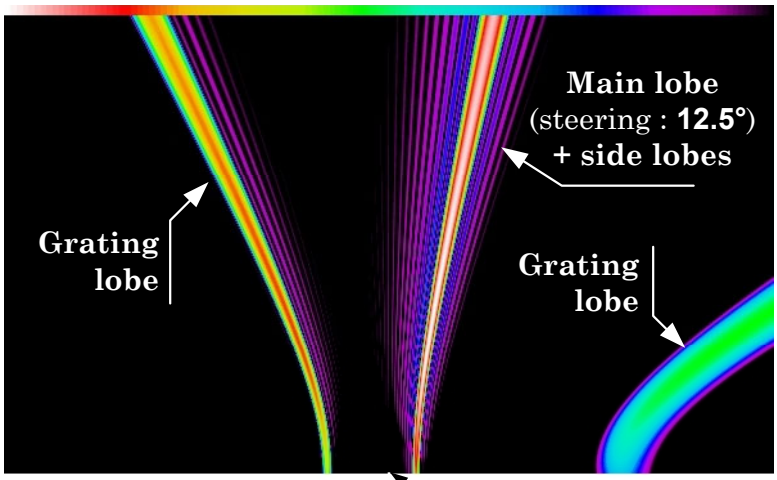

LINEAR RECEIVING ARRAY (c)

Figure 1.21 : 3-D diagrams. a) Torus ; b) Arc of a circle ; c) Linear array

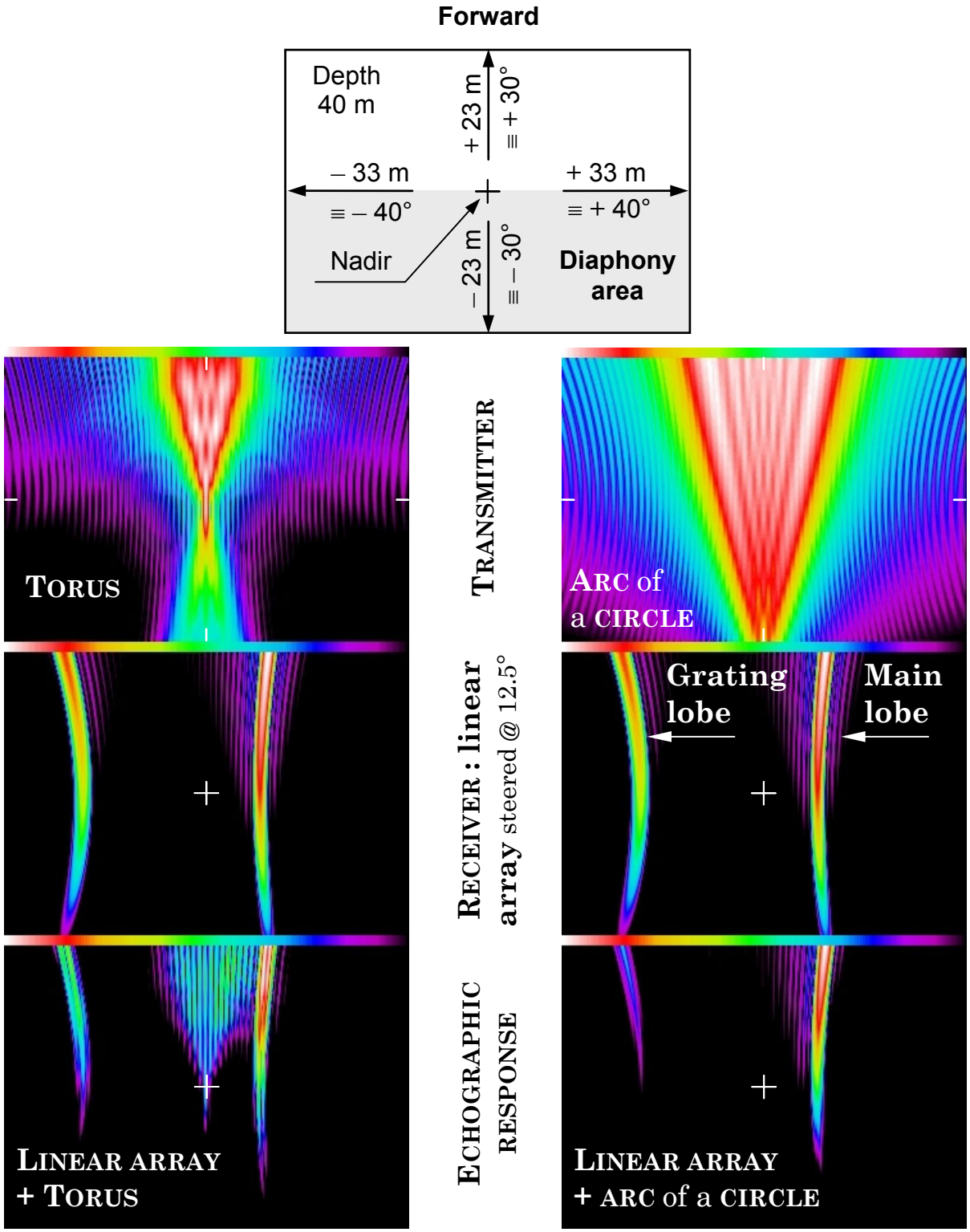

Figure 1.22 : 3-D diagrams zooming on the nadir area.
Left part : Torus ;
Right part : Arc of a circle

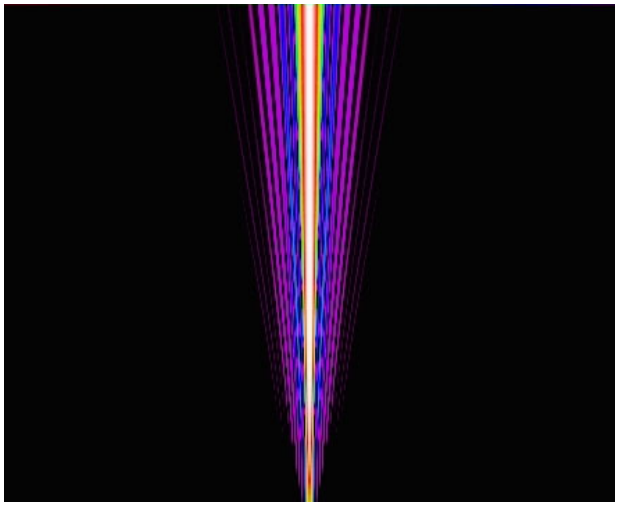

Steering 0°

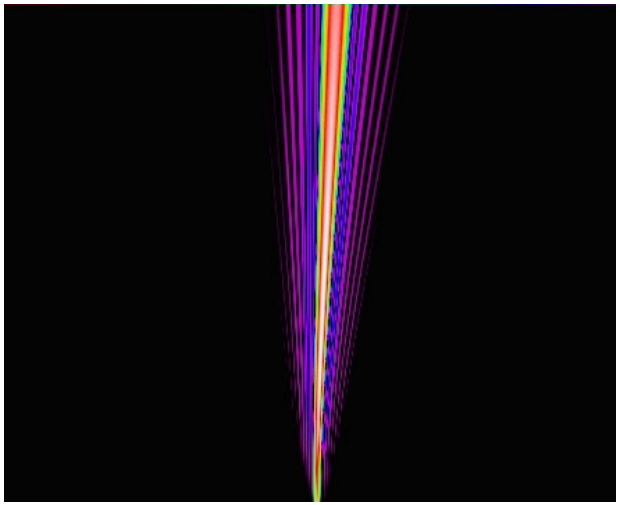

Steering 3°

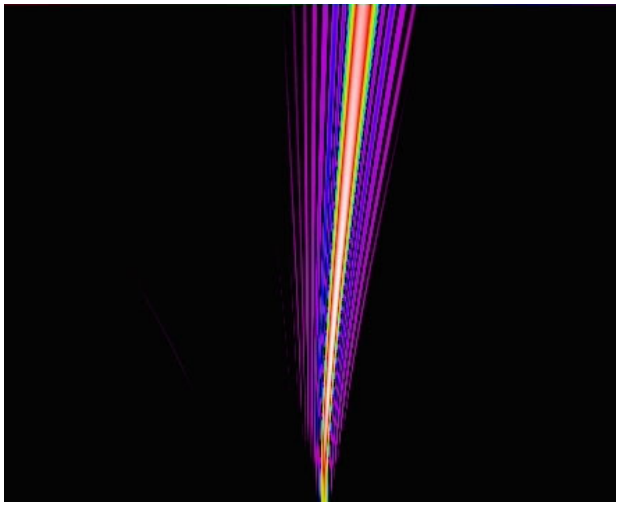

Steering 6°

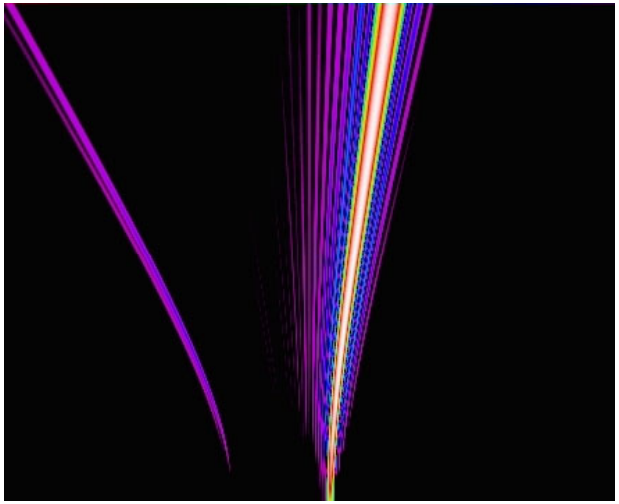

Steering 9°

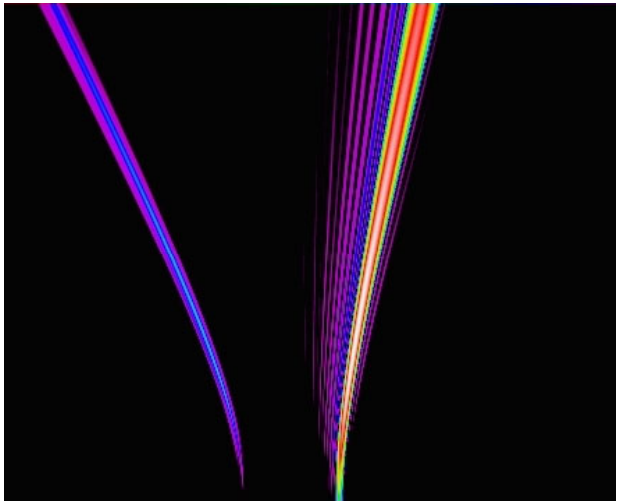

Steering 12°

Figure 1.23 : Echographic diagrams

0 to –40 dB

FIELD @ 40 m depth
- Nadir to 150 m ahead, i.e. 0° to 75°
- Lateral extent : – 92 m to + 92 m

TRANSMITTER : Arc of a circle
- Curvilinear length : 80 cm
- Radius of curvature : 1.4 m
- Axis slanted @ 40°

RECEIVER : Linear array (32 elements)
- Length : 72 cm
- Axis slanted @ 40°
- Taper window : Truncated Gaussian (20% at ends)

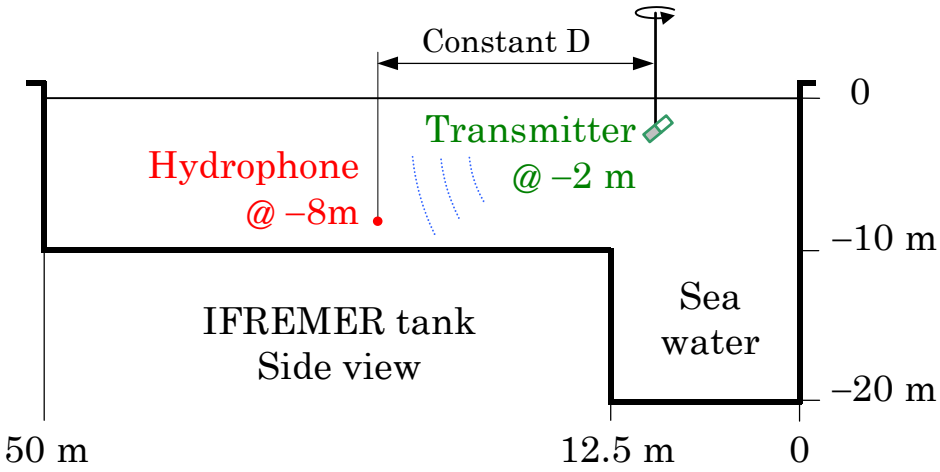

Figure 1.24 : Configuration #3 at the IFREMER's tank.
Measurement of diagrams at constant grazing angle
Revolution axis of the transmitter slanted 40° / vertical
Given distance D, the transmitter is rotated around a vertical axis

It must be noticed that beam steered angles (at receive) are different than azimuth angles as referenced in Figures 1.25. Azimuth angles denotes the orientation of a vertical plane. Considering constant grazing angles (referenced to the horizontal plane) and constant ranges, the diagrams drawn in the latter figure corresponds to locus on a cone whose axis is vertical. Hence, it is normal that the aperture becomes larger as the grazing angle increases. At the limit given by a grazing angle of 90°, the diagram becomes flat over a 360° azimuth extent. From an experimental point of view, it was much easier to check the beam pattern of the transmitter as presented. It can be seen that the measured diagrams fit reasonably well with the theoretical expectations.

The efficiency of the transmitter measured along the main axis is found to be around :

SV = 151 dB ref. 1µPa @ 1m / V

The power amplifier feeds the antenna with about 1300 V_{pp}, which gives a source level larger than **204 dB ref. 1µPa rms @ 1m**.

Compared to a possible more sophisticated shape, the arc of circle gives a lesser rejection of echoes that come from the surface, as well as from behind the across-track plane. However, it must be noticed that this geometry still yields the same kind of diagram to this respect as any side scan sonar system.

The active surface is also smaller than with an hypothetical optimized torus, but the obtained level remains sufficient to gather data at a range that reaches a few hundred meters.

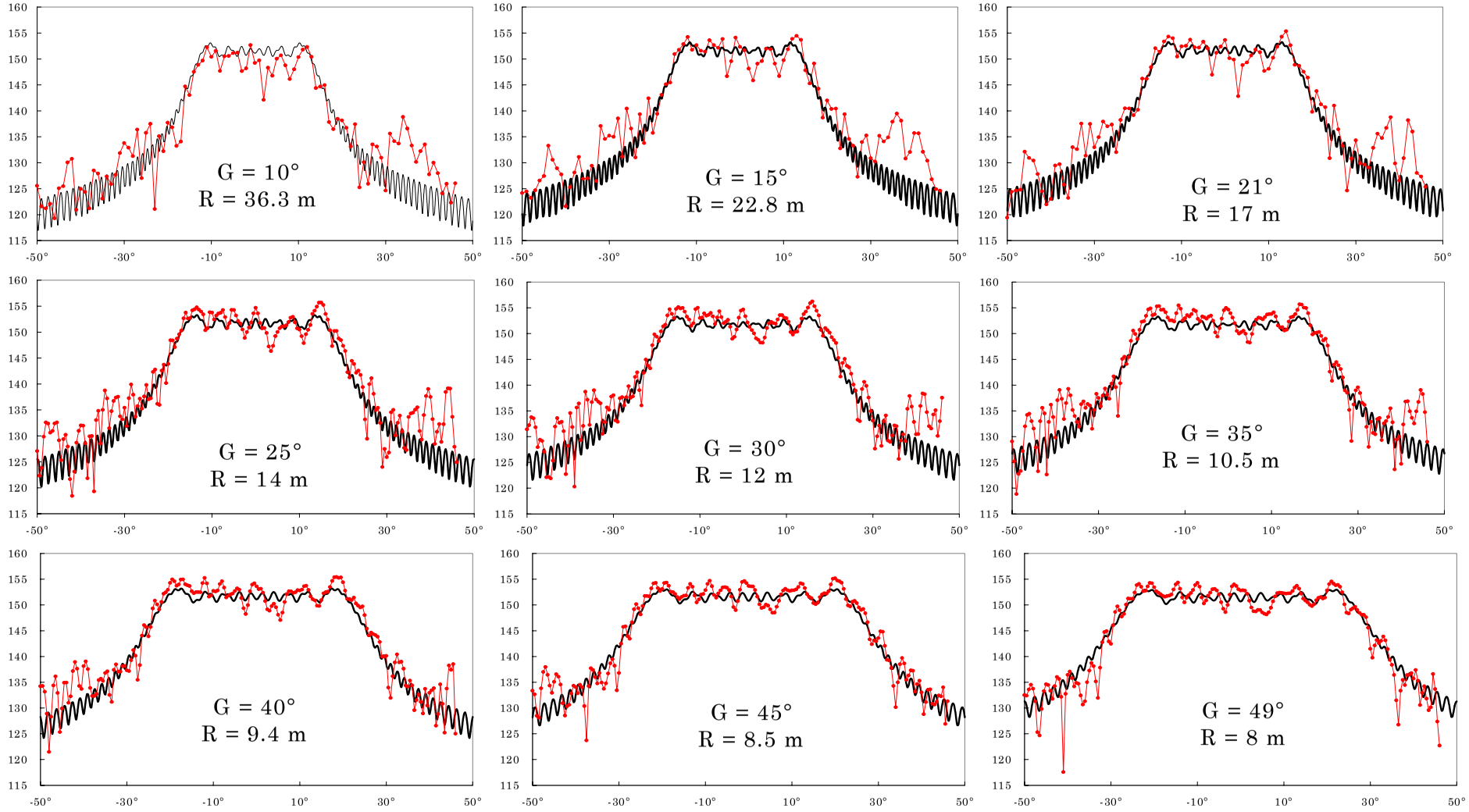

Figure 1.25 : Experimental and numerical diagrams at constant grazing angles and ranges
Y axis : SV in dB ref. 1µPa @ 1m / 1V (scale from 115 to 160 dB)
X axis : azimuth from –50° to 50°

1.5 STATISTICS ON THE WHOLE SURVEY

The transmitting antenna insonifies a large solid angle. In order to generate the required power and to cover the proper 3-D sector, the shape of the antenna is such that at least one dimension is much larger than the wavelength. With this geometry, the resulting field cannot be anything else than "bumpy". It is necessary to compensate for this lack of homogeneity when exploiting the data collected with the system, e.g. for building images or for deriving information of the angular response of the seafloor. It is not realistic nor reliable to attempt a complete measurement in tank of the spatial response of the antenna. A more convenient way is to derive such an information from statistics performed on data gathered at sea. Keeping in mind that the reflectivity of the bottom versus the grazing angle is a critical information to characterize the seafloor, the chosen angular referential used to perform the calibration is made of : 1) the steering angles ; 2) the grazing angles.

At a post-processing stage, the level of beamformed data is corrected for the geometrical spreading and attenuation losses versus range. Considering a single ping, the range of the first bottom detect is searched. Grazing angles are assigned to each beamformed data according to a flat bottom assumption.

Let us denote $I^2(p, b, g)$ the resulting energy of the compensated echoes, where p is the ping index, b is the beam index, and g is the grazing angle. Statistics are performed on all pings of the survey in order to derive :

$$R^2(b, g) = < I^2(p, b, g) >_p$$

This mapping is split into two parts according to :

$$R^2(b, g) = \gamma \, A^2_g(b) \, G^2(g)$$

where $\gamma = < R^2(b, g) >_{b,g}$ is a normalization factor, and $G^2(g) = < R^2(b, g) >_b / \gamma$

Figure 1.26 displays the normalized echographic response versus the beam index given by $A^2_g(b)$. This surface can be used to compensate for the artefact caused by the system, but without introducing any change in the response in site. The so corrected data are suitable for studies addressing seafloor characterization.

In the compound imaging process, echoes incoming from various grazing angles are merged. It is therefore necessary to equalize the levels of these echoes by taking into account the additional normalized compensation given by $G^2(g)$, that is displayed in Figure 1.27.

Note that the main archives do not take into account the above described compensation. This is because the statistics are performed with the flat bottom assumption for each ping : Such statistics may eventually be improved by taking into account the actual relief of the seafloor derived by means of the interferometer.

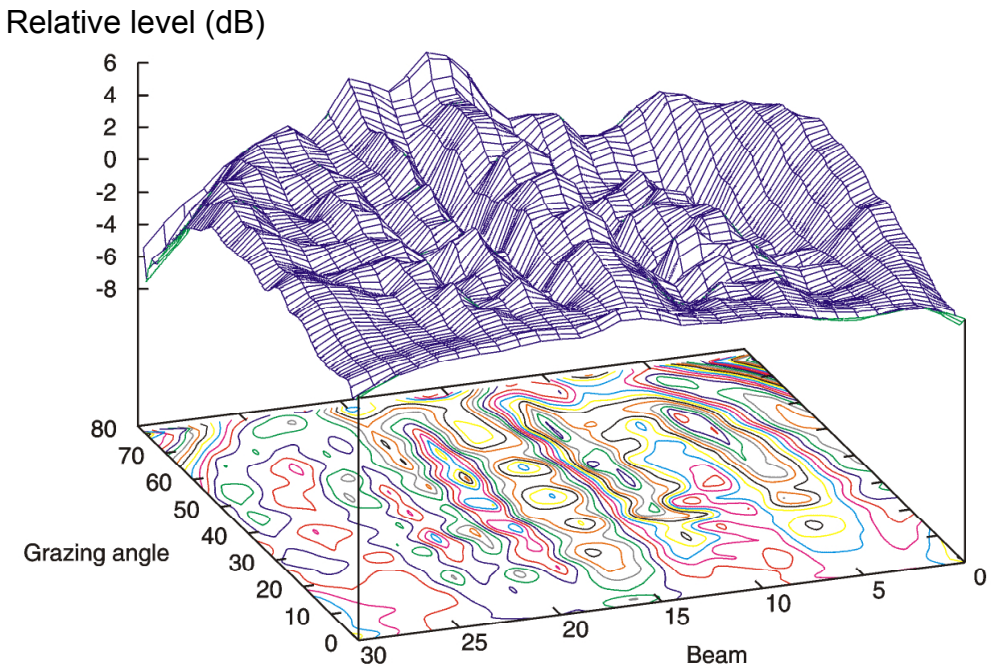

Figure 1.26 : Echographic response in azimuth for various grazing angles

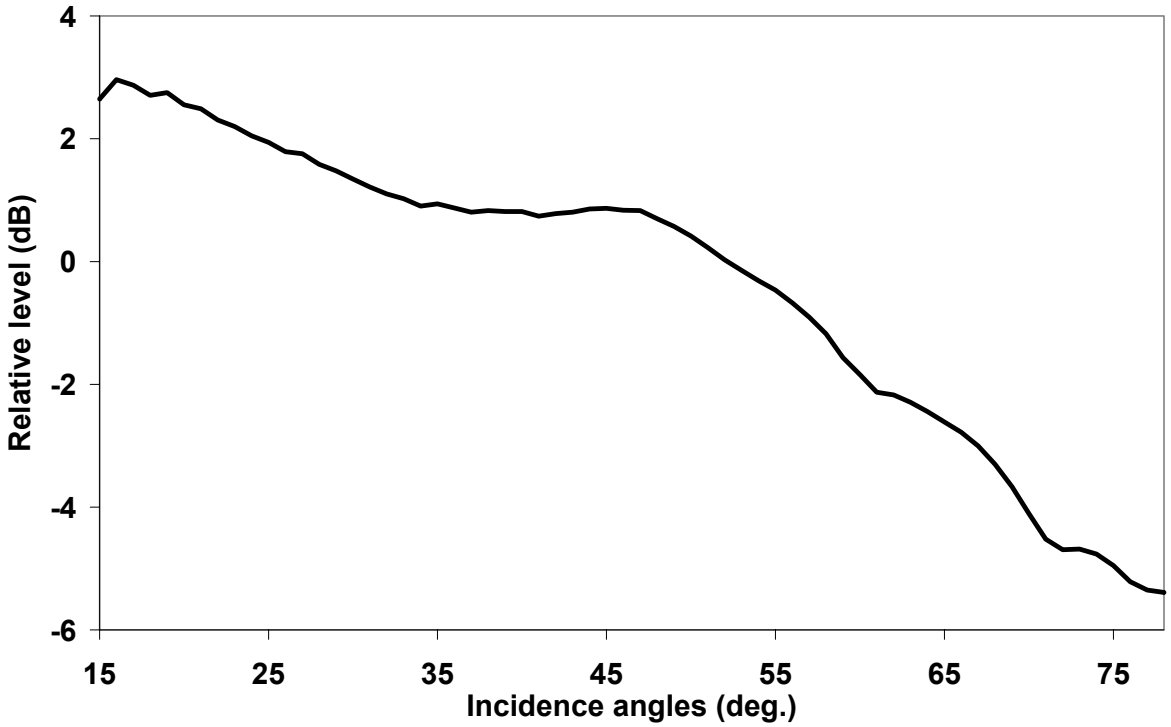

Figure 1.27 : Dependence in site of the mean echographic response

2. ELECTRONICS AT TRANSMIT AND AT RECEIVE

2.1 GENERAL DESCRIPTION

The electronics of the sonar system is designed to achieve the following goals :

- Generation of a powerful FM signal to the transmitter.
- Output of digital data corresponding to : 1) The echoes received by each elementary transducer (for post-processing purpose) ; 2) Preformed beams (for in-line display and control).
- Controls of the whole sonar system.

The electronic system is divided into two parts (Figure 2.1) : The wet module and the surface unit, that a 50 m long ombilic links.

The wet module (Figure 2.2) consists of :

- The antennae with the front-end electronics that is embedded in the receiving arrays ;
- A container whose included electronics
  - exchanges control information with the surface unit,
  - forwards the power signal to the transmitter,
  - inputs analog multiplexed signals from the receiving antennae,
  - outputs acoustic serialized digital data to the surface unit.

The surface unit (Figure 2.3) can be divided into three parts :

- Transmitted signal generation and power amplifier
- Digital processing of transducer data to derive beamformed data
- Hardware control of the system

A PC is interfaced to the surface unit, in order to store the incoming stream of acoustic data, and to provide high level controls. Another PC gathers and stores information provided by the onboard instrumentation.

Electronics at transmit and at receive (Task 2.2) is described in the present section. The setup used for data storage, system controls and displays (Task 2.3), is described in Section 3.

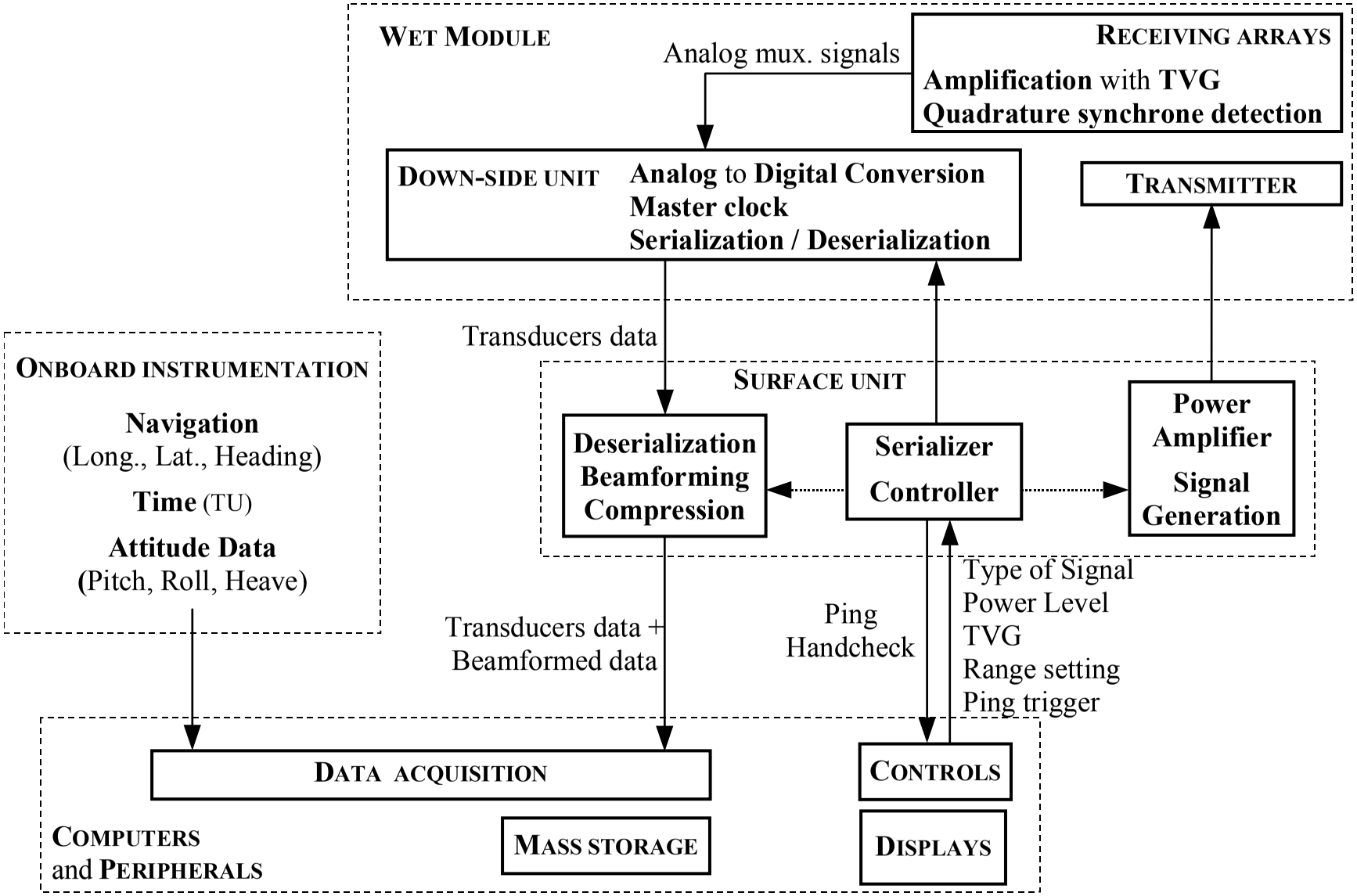

Figure 2.1 : Scheme of the system

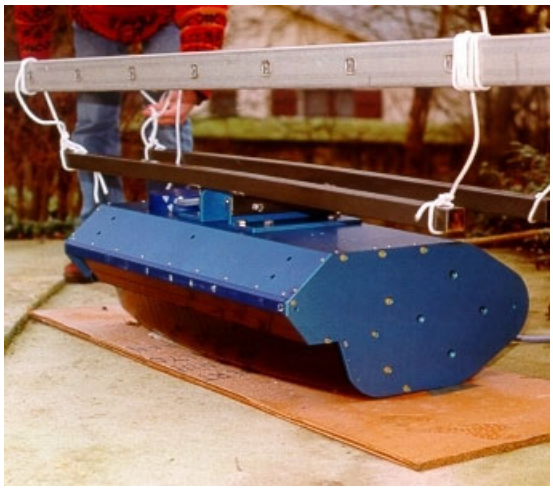

Figure 2.2 : Wet module

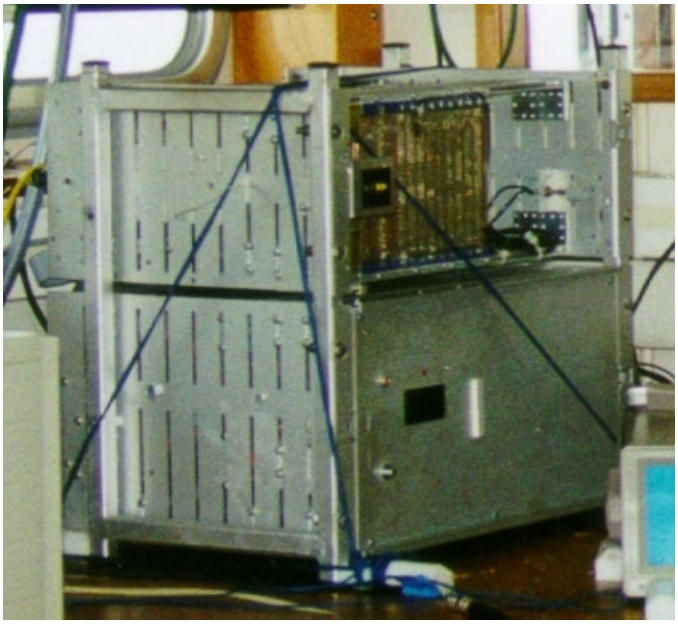

Figure 2.3 : Surface unit
Upper part : Digital processing
Lower part : Power amplifier

2.2 WET MODULE

2.2.1 Electronics embedded in the receiving arrays

Two identical linear arrays are used at receive. Electric signals issued from the 2×32 elementary transducers are first amplified with a Time Varying Gain (TVG), then basebanded (quadrature synchronous detection) and filtered, before being digitized. The whole analog processing is performed with a front-end electronics that is directly embedded in the antennae (Figure 2.4), so as to minimize the noise that can rise at this stage. Each array contains 8 cards ; Each card processes 4 transducers (Figure 2.5-6). The scheme of an elementary demodulation unit is displayed Figure 2.7.

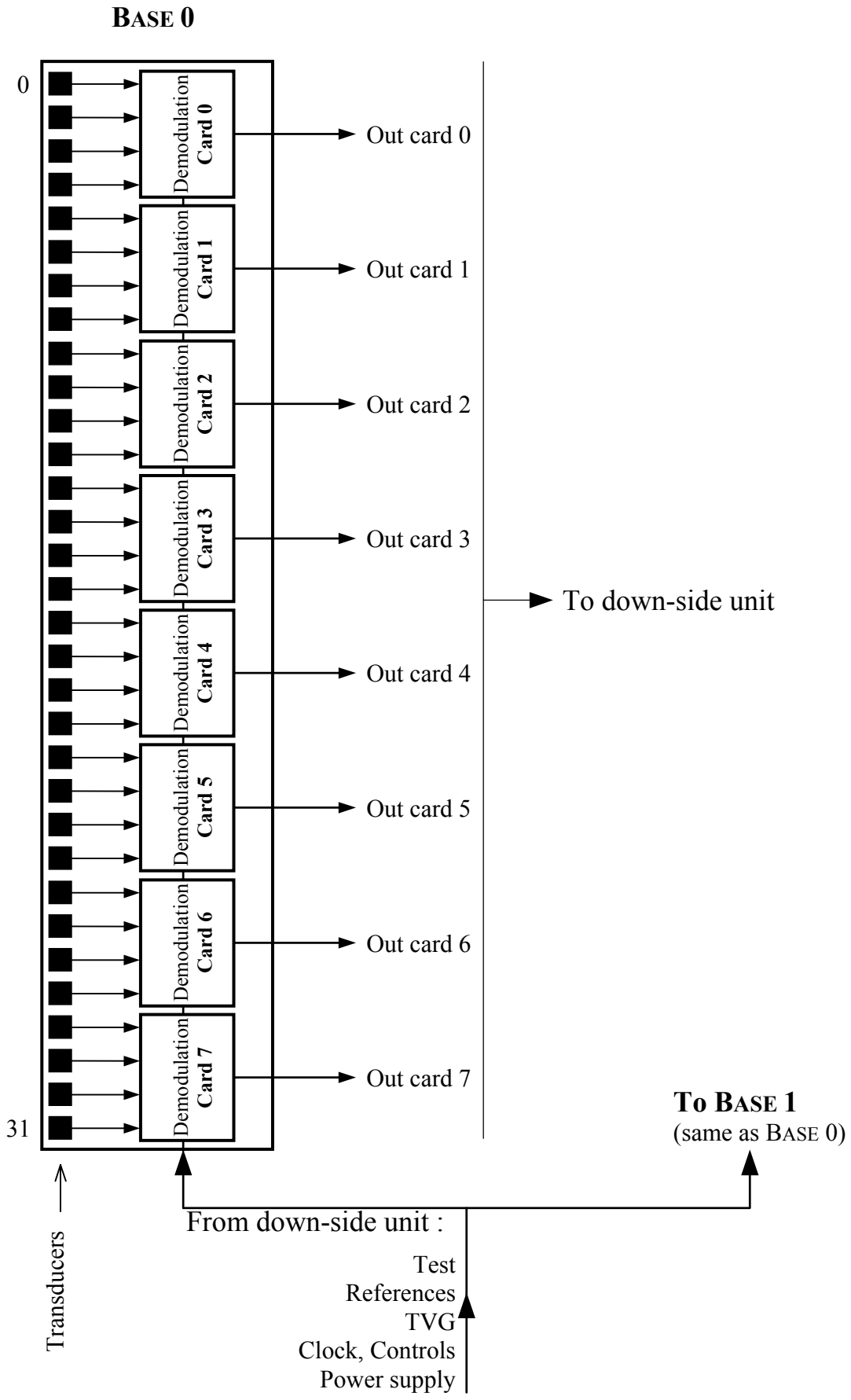

Figure 2.4 : Scheme of the demodulation cards embedded in the receiving arrays

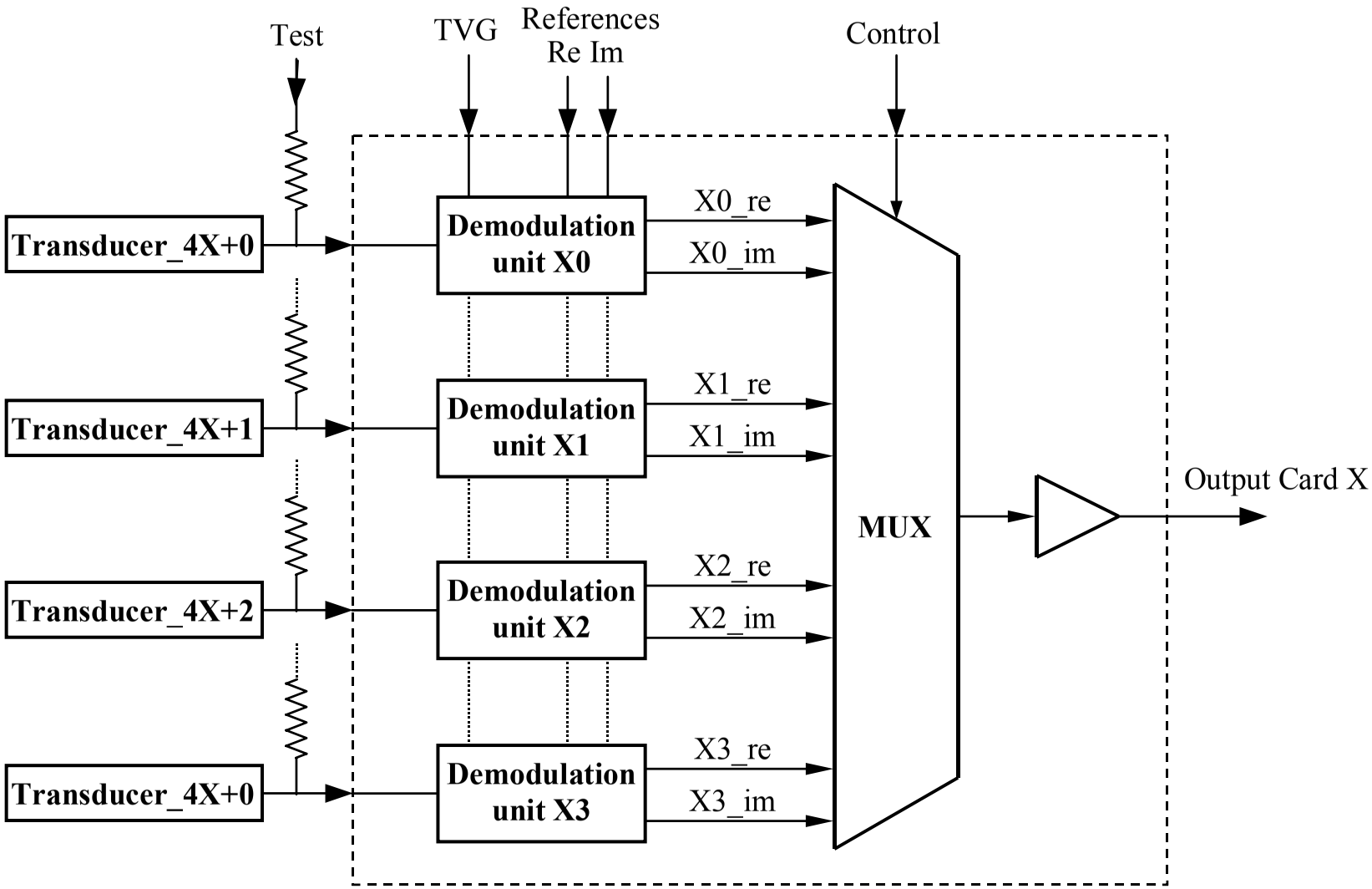

Figure 2.5 : Scheme of a demodulation card

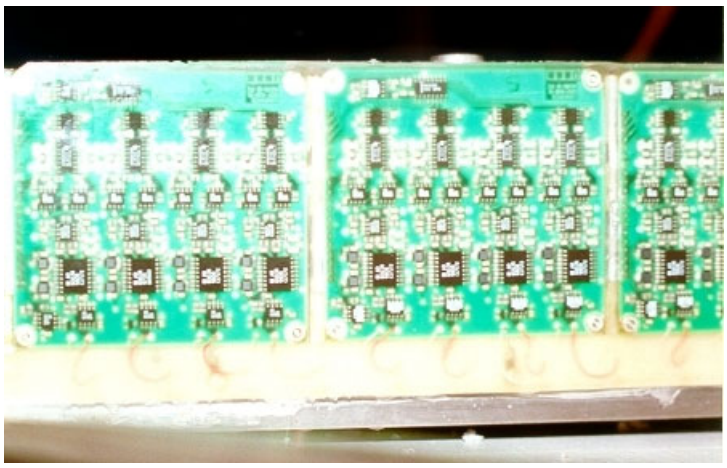

Figure 2.6 : Demodulation cards

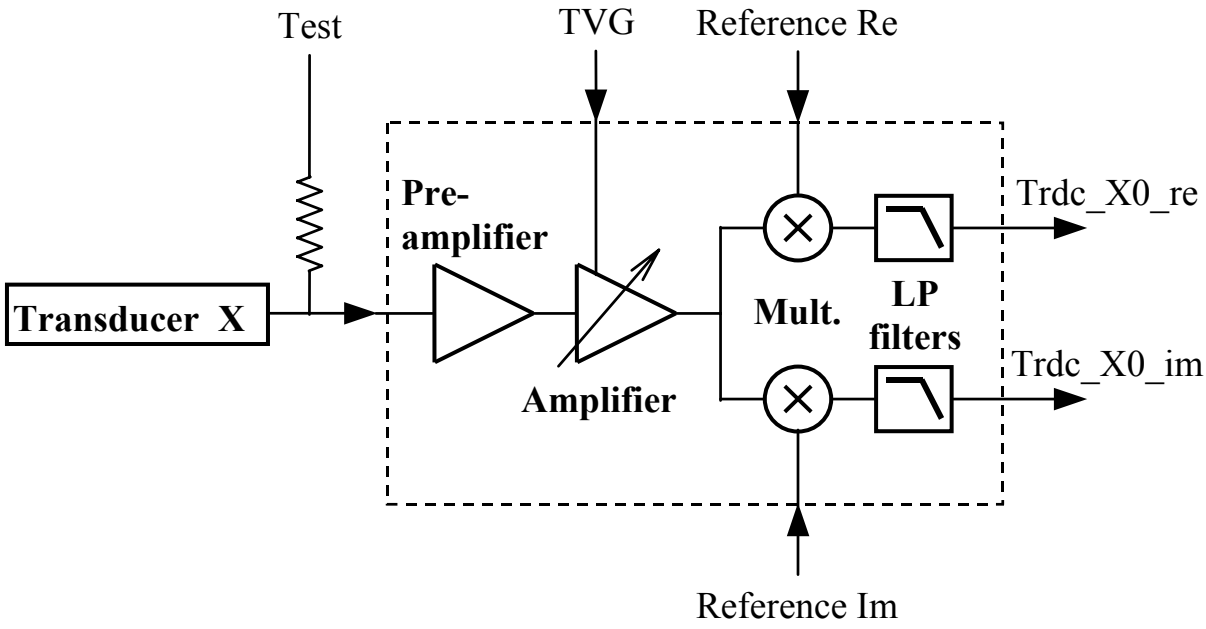

Figure 2.7 : Demodulation unit (4 units per demodulation card)

Each array is fed with lines that carry :

- the power supplies,
- clock and multiplexing controls,
- a signal that drives the TVG amplifiers (about 80 dB dynamic)
- the reference signals needed for baseband demodulation (100 kHz in quadrature)
- a test signal that can simulate the transducer responses in order to check the functioning of the whole system, including the acquisition stage.

The 4 × 2 analog outputs of the 4 demodulation units that each demodulation card contains are integrated, then hold and multiplexed (Figure 2.5) with a recurrence cycle of 256 µs (about 4 kHz). Hence, each array outputs 8 lines (Figure 2.4) that carries the multiplexed analog base-banded signals to the container located close behind the antennae.

2.2.2 The down-side unit

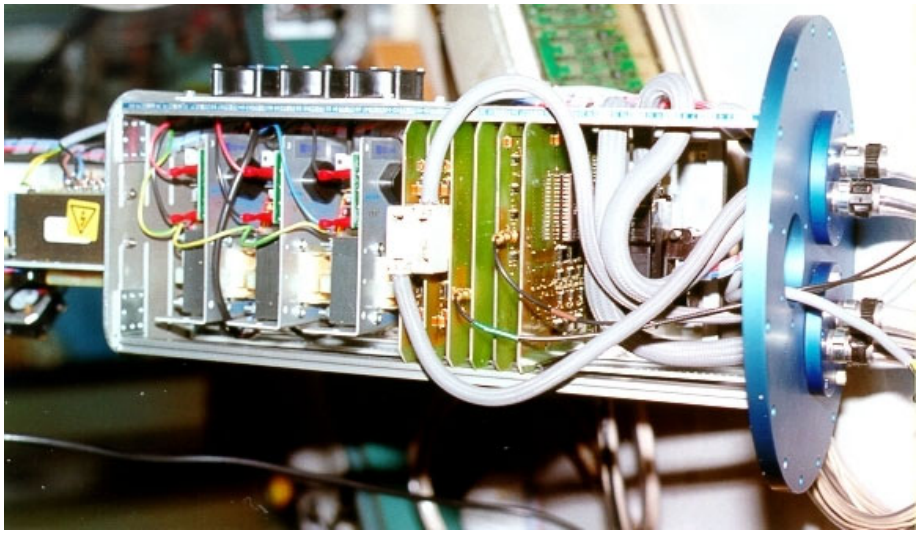

Figure 2.8 : Downside unit with power supplies

Figure 2.9 displays the functional scheme of the down-side unit. The multiplexed signals received from the antennae are digitized with 12-bits converters (one DAC per line) working at 32 kHz (8 × 4 kHz). All the outputs of the converters are then serialized, expanding 12-bits data to 20 bits in order to allow the logical control of the data flow at receive by the surface unit. The required throughput of the up-link serial line is thus :

2 bases × 32 transducers × 2 quadrature samples × 20 bits × 4 kHz ≈ 10 MHz

Actually, the bandwidth of the line is 20 MHz and the duty cycle is halved. The downside unit includes the 20 MHz master clock of the whole system. The serial line is referenced to a neutral electrical level, i.e. logical 1s are transmitted with positive pulses, and 0s with negative pulses. Doing so, the master clock is continuously transmitted, together with data, to the surface unit.

An input serial link transmits the orders from the surface, including :

- Update of the Time Varying Gain law. The down side unit stores the digital values. Then, the unit converts this 7-bits data stream into an analog voltage supplied to the receiving arrays for controlling the amplifiers' gain.
- Range setting, i.e. duration of the receiving activity
- EXTERNAL or INTERNAL ping trigger. In INTERNAL mode, the recurrence of the ping is a constant that depends on the range setting. This mode was mainly used during the development of the prototype. In EXTERNAL mode, ping trigger is controlled by software at the surface. During the surveys, the latter mode has been preferred as it warranted that enough time was allowed to achieve the software management (displays, controls, storage).
- Ping trigger, i.e. beginning of the receiving activity in EXTERNAL mode
- NORMAL or TEST mode of operation. In TEST mode, the test pattern stored in EPROMs is converted to an analog signal that feeds the front-end electronics.

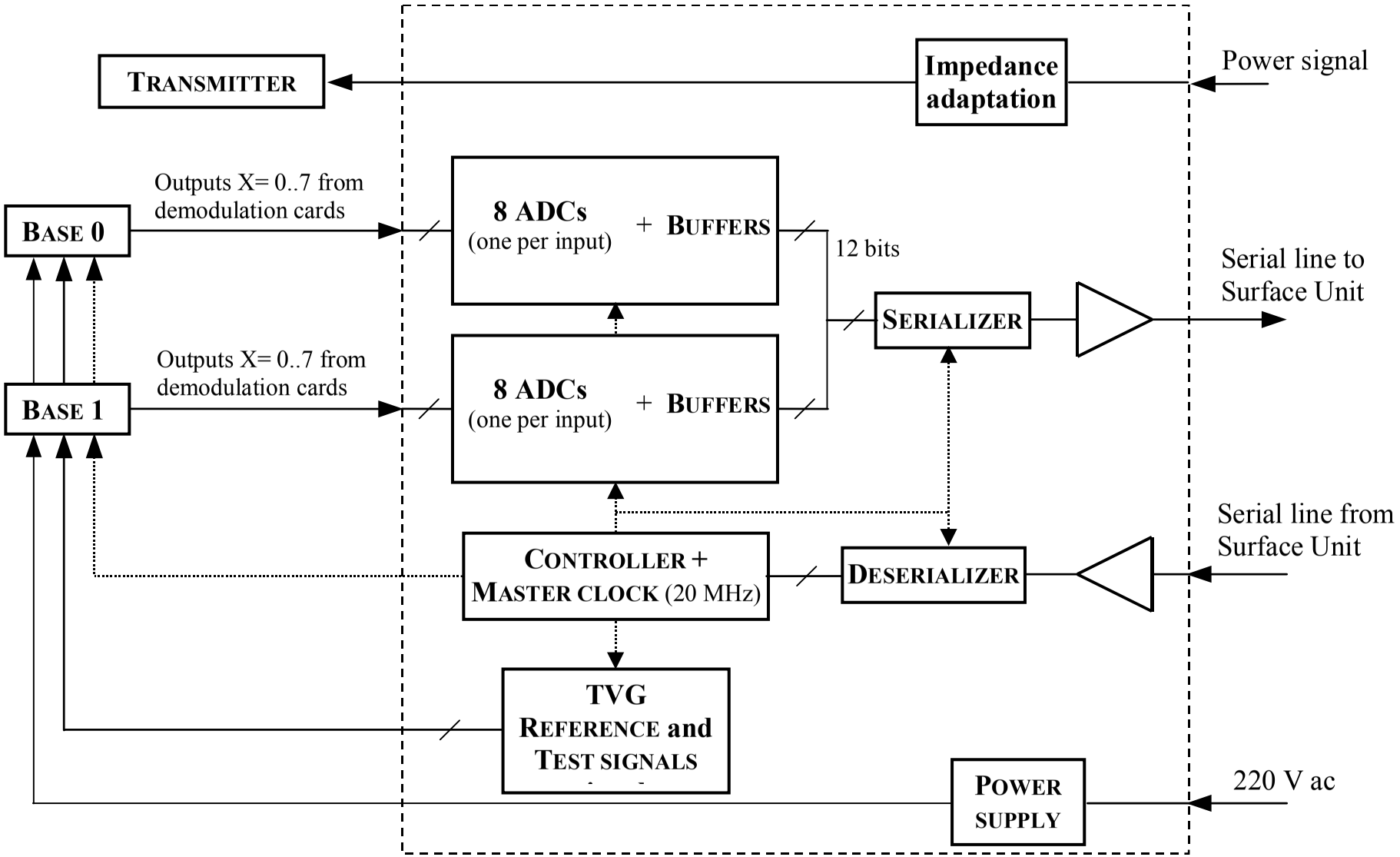

Figure 2.9 : Scheme of the downside unit

2.3 SURFACE UNIT

2.3.1 Transmitter electronics

The signal patterns used at transmit are stored in EPROMs. During normal mode of operation, the only signal used is a Chirp :

- Central frequency : 100 kHz
- Linear frequency modulation : 3 kHz
- Duration : 8 ms
- Gaussian envelope truncated at 20% of max amplitude at ends

When a ping is triggered (either in INTERNAL or EXTERNAL mode), the 8-bits digital data are read and converted at 5 MHz sampling rate into a low voltage analog signal that drives the power amplifier.

The power electronics is based on a pair of push-pull amplifiers. The signal level is adjusted according to the requested setting (attenuation of 0 dB, -10 dB, -20 dB or -30 dB). An analog tuning (potentiometer) is also available. During the survey, the maximal level was always chosen. Driven with the nominal Chirp recorded in EPROM, the output voltage reaches about 1300 Vpp. The reactive load is about 200 Ω, so that the amplifier delivers more than 1 kW *rms*. Limiting the transmitted power at such a level is intended to insure a linear response of the amplifiers. In TEST mode, there is no driving signal sent to the power amplifier. (Actually, the amplifier should be switch off when using this mode).

A spare power amplifier has been built (but not used) in order to limit the risk of failure during the data acquisition at sea.

2.3.2 Digital processing and controls

After ping trigger, the surface unit (Figure 2.10) receives data from the downside unit via the uplink serial line for a duration that depends on the range setting. The 20 MHz master clock is recovered. The boundaries of packets corresponding to transducers data belonging to the same 256 μs time sample are identified. A "tixel" address is generated to tag the beginning of each such packet. Data from the first tixels of each ping are used to evaluate the offset biases that rose in the digitization process. The remaining incoming data are compensated in-line for the offsets so found in each channel.

Past the offset removal, transducers data enter a dedicated digital circuitry that performs beamforming and pulse compression. The beamforming is achieved with a dynamic focusing based on the Fresnel law. Transducer data can be tapered (Truncated Gaussian law) or not, depending on the control settings. Eight focal zones and 2 × 31 directions are taken into account. Pulse compression is performed with the complex, basebanded replica of the transmitted chirp, stored in EPROMs (time sampling : 256 μs).

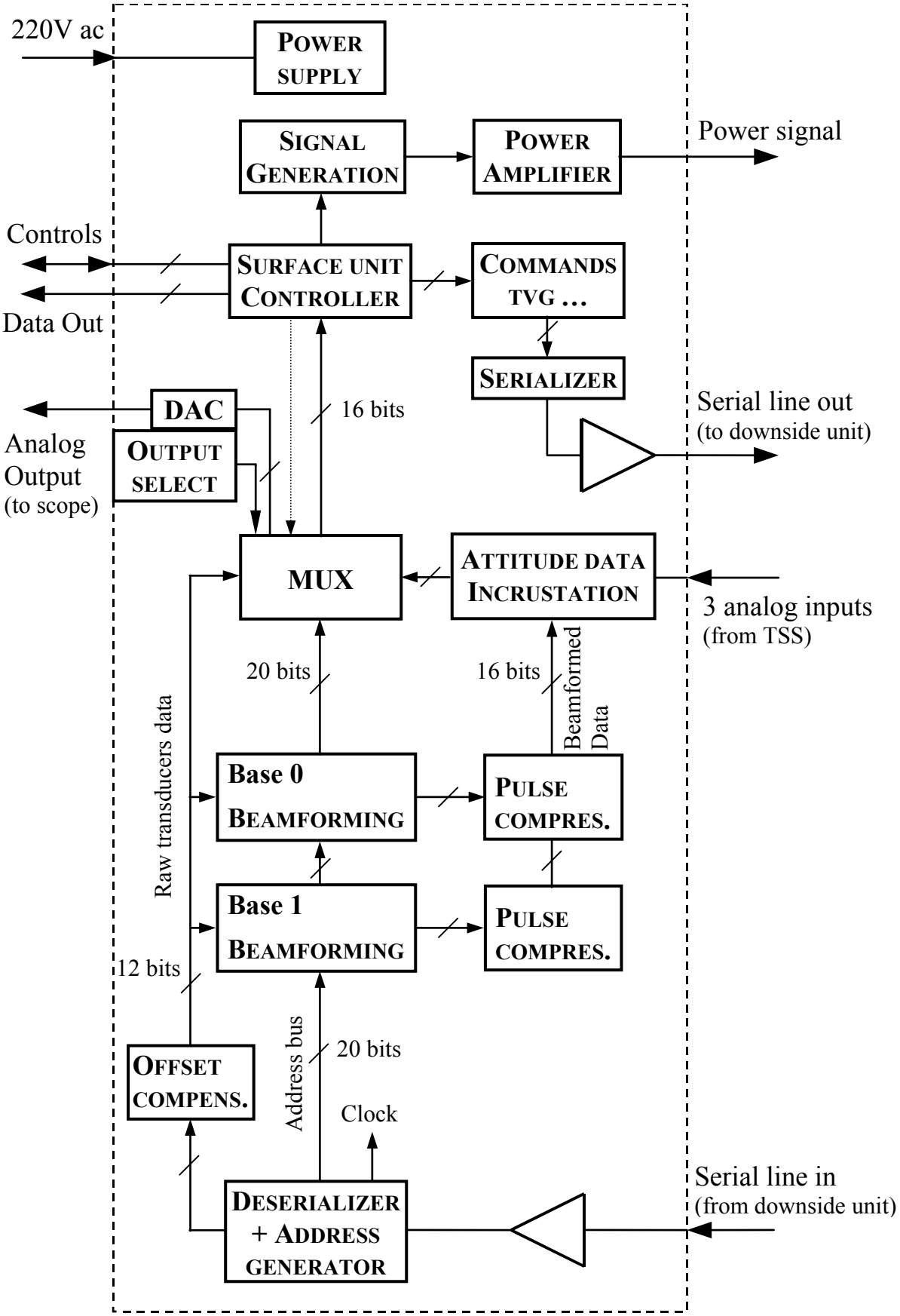

Figure 2.10 : Functional scheme surface unit

A multiplexer gathers both transducers and beamformed data on a 16-bits wide output bus (12-bits transducers data are expanded to 16 bits). This bus transfers 256 16-bits words per tixel to the acquisition board installed in a PC. One tixel is sampled every 256 µs so that the digital throughput is equal to 2 MByte/s. There are 128 words, i.e. 2 × 32 complex values made of 2 words each, reserved for the transducers data, and 128 words for the beamformed data. Because only 2 × 31 beams are actually computed, 4 words remain free to carry miscellaneous information such as the tixel address and attitude data : The surface unit features 3 analog inputs that were connected to the Vertical unit TSS during the sea trial. Roll, pitch and heave signals are digitized and embedded in free slots of the output data stream. Note that digital attitude data directly output by the TSS unit were otherwise recorded by another PC ; Attitude data incrusted in the sonar system output are only used for testing purpose and future developments.

An analog output allows to observe directly with a scope the content of any of the 256 digital output channels. The channel is selected manually, with a set of 4 rotating switches.

When the delay allotted for receive is expired, the system enters a wait order state. The duration of this state is fixed (64 ms) in INTERNAL mode, or extents to the next ping trigger in EXTERNAL mode. During this period, orders are received by the surface unit controller, and serialized to feed the slow down-link line that transfers the information needed by the wet module (see the previous description of the down-side unit).

Figure 3.1 displays a scheme of the connections that link the main components of the COSMOS prototype. Note that the serial links that connect the surface and the downside units are made of two single coaxial cables. The previous sections described what has been identified as the "electronics" of the system. The next section focuses on the interfaces that manage the sonar operational controls and data storage.

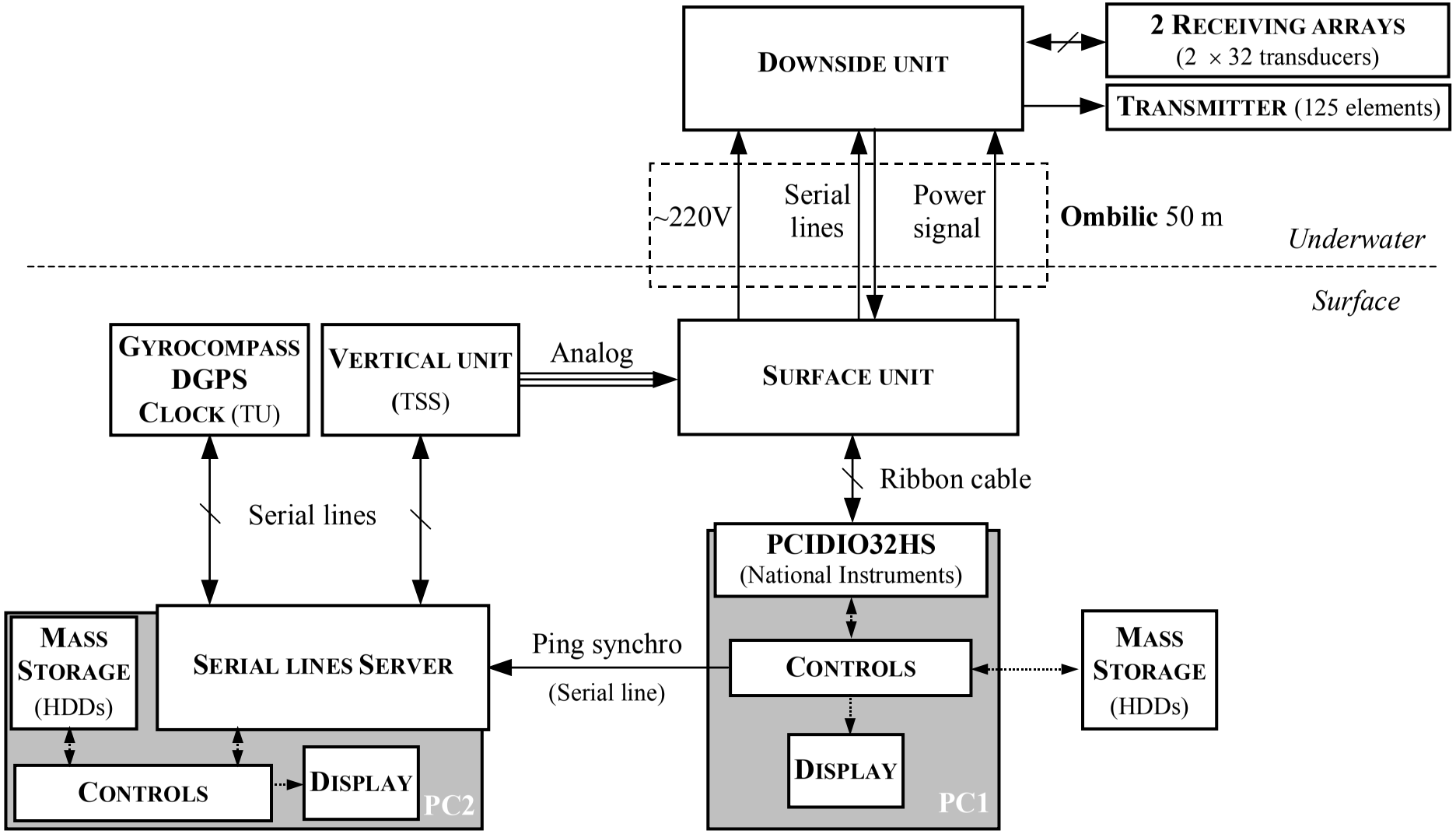

Figure 3.1 : Scheme of the connections between the units of the system

3. DATA LINKS AND STORAGE, SYSTEM CONTROLS AND DISPLAYS

3.1 INTRODUCTION

The main objective of Task 2.3 was to insure the proper recording of data collected during the sea trials, including the control of the sonar. Part of the challenge came from the large amount of the acoustical data to be recorded and displayed in-line, together with the variety of other sources of data (attitude, navigation) : Assuming a ping cycle of 1 s and a typical maximal slant range of 500 m, a one-hour survey implies roughly 5 Gbytes to be recorded. The task includes also the transfer of the recorded data on a convenient, reliable support for diffusion to users and archiving purpose.

The original plan was to collect the acoustical, navigation and attitude data with a single PC platform. TEISA designed and developed an industrial oriented architecture, working on this scheme until the end of the second year of the contract. More details, as well as a description of the encountered difficulties, are given in the report from TEISA appended to the present report.

LMP and TEISA foresaw at the end of the third semester that this solution could not be ready for the sea trials. Therefore, an alternative solution based on using two PCs was developed concurrently with the ongoing initial plan. Since the beginning of the project, LMP developed an acquisition unit in order to test the prototype under construction. This system is based on using a PC with a *National Instruments* acquisition card (PCI-DIO32HS). Originally, the setup merely enabled to record individual pings on the PC Hard Disk. Fortunately, the acquisition card proved to behave enough friendly with the Windows 98 operating system. So, LMP extended the role of the unit to the operational (i.e. continuous) collection of the acoustical data, and to the complete control of the sonar. In Figure 3.1, PC1 and PC2 denote the contributions of LMP and TEISA, respectively, in the final setup. This configuration worked fine during the sea trial : All data were properly recorded, together with a correct control of the system.

3.2 GENERAL DESCRIPTION

The PCI-DIO32HS acquisition card enables parallel exchanges of data over 2×16-bits wide bus, with a sufficient throughput with regards to the requirement of the present application (1 Mword/s). Annex 1 describes the proprietary sonar bus. The critical issue was the amount of resources that this card and its associated drivers leave available for the PC to handle simultaneously other tasks. Finally, a stable behavior could be reached, without degrading the ping rate.

Two processes are initiated on PC1 for operating the sonar system. A master program is in charge of :

- Data acquisition, checking and storage ;
- Sending orders to the sonar electronics ;
- Building the bitmaps for data display.

The second process displays the images, and manages the control combos that allow the operator to define the sonar settings (type of signal, source level, maximal range, TVG…).

Two buffers are reserved in the central memory of PC1. Each buffer is large enough to hold an entire acoustical set of data produced during one ping. The main sequence of operations is described in the following, starting at ping trigger controlled by the master program.

- A synchronization message is send to PC2.
- The PCI-DIO32HS starts to write incoming data in one of the buffers.
- In the meanwhile, the other buffer which holds data of the previous ping is dumped into external SCSI hard disks (3 × 18 GByte). The management of the mass storage space and of the change of drivers is automatic, allowing a seamless recording.

The latter transfer is completed well before the end of the acquisition process. This leaves enough time :

- to display, in a secondary window, the TVG curve together with the upper envelop of the signals received on the antennae ;
- to build a sector image of the beams (formed from either base) ;
- to build the echogram corresponding to the raw acoustic levels received by all the elementary transducers.

Then, the master program leaves the control to the second process :

- The displayed images are updated ;
- The changes of settings that could have been entered by the operator, including display controls, are loaded ;

This process gives back the control to the master program :

- The acquisition card is polled to detect the completion of data receiving ;
- Afterwards, the newly acquired data set is checked for consistency ;
- The updated orders are sent to the sonar electronics ;
- Finally, the addresses of the two buffers are swapped before iterating the whole procedure. A 1 ms accurate timer allows to trig pings at regular intervals.

The second platform (PC2) features a serial ports server that allows to collect navigation data (from DGPS and gyrocompass) and attitude data (from the TSS unit). These data are stamped with the internal clock of PC2 before being stored on hard disks. All the serial line inputs are continuously monitored, and the collected information (ship route, attitude, …) are displayed in-line by means of the surveying tools developed by TEISA. At each ping transmit, PC1 send a message to PC2 (via a serial link) where the local time stamp is also appended. This procedure enables the synchronization of all the collected information at the merging, post-processing stage.

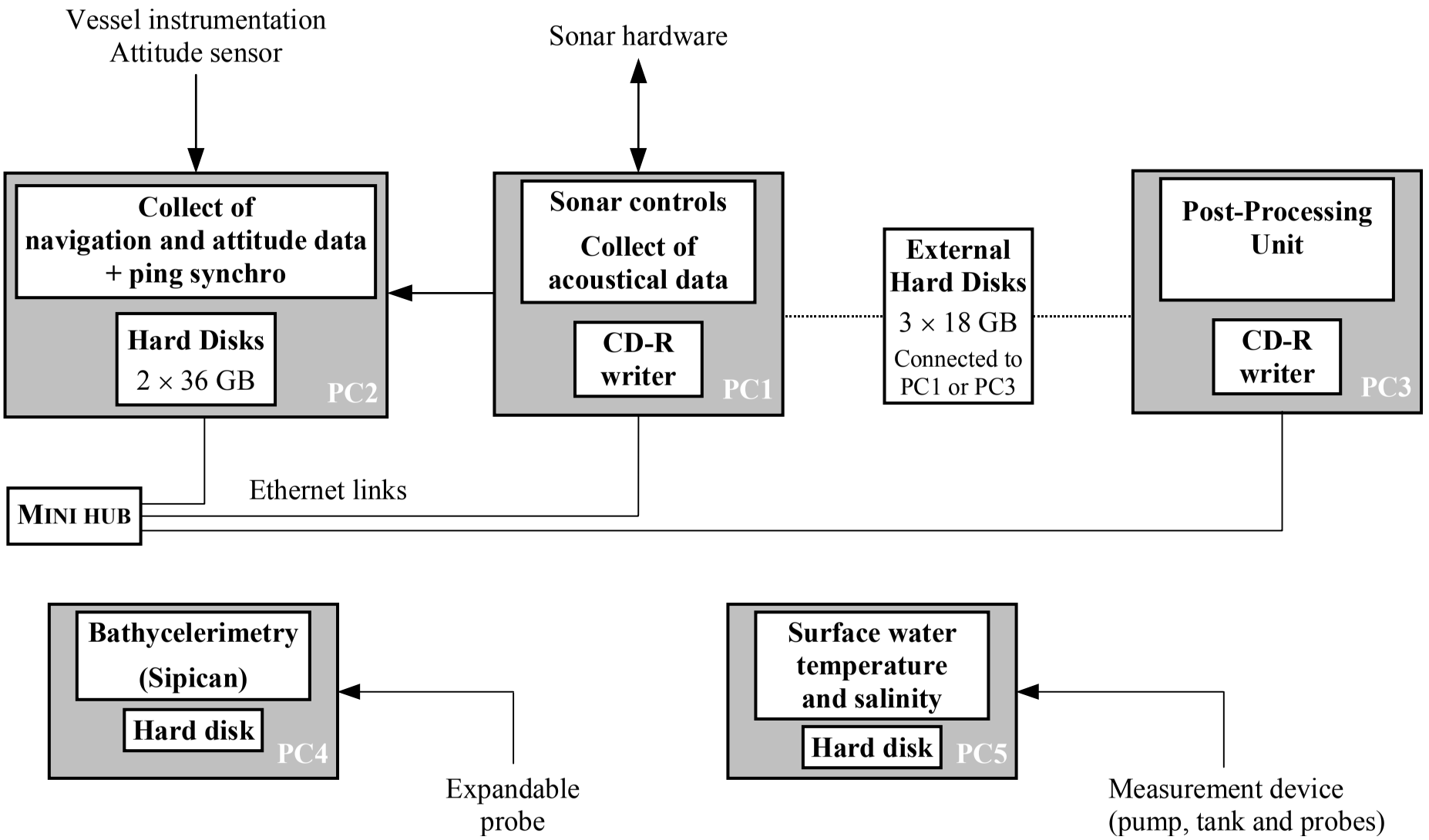

Figure 3.2 : Scheme of the computers and peripherals dedicated to data acquisition

Figure 3.2 displays the scheme of all the computers and peripherals dedicated to data acquisition during the sea trial. Bathycelerimetry profiles were recorded twice a day with an autonomous SIPICAN unit. Another autonomous unit recorded continuously, at a slow rate, the temperature and salinity of water in the vicinity of the shiphull. The corresponding amount of data collected during four days was small enough to be transferred by means of diskettes.

3.3 DATA MANAGEMENT

About 100 GB of data were collected during the four days that the survey last in the vicinity of the Barcelona. The capacity of the hard disks connected to PC1 is large enough to hold acoustic data collected during one day. At night, at least one disk was unmounted and connected to PC3 – another computer used for post-processing. Both PC1 and PC3 are equipped with CD-R writers so that all data collected during the day could be saved on compact disks. All the recorded CDs have been checked.

In addition, PC2 carries two large hard disks (2 × 36 GByte). A local Ethernet network connected PC1-2-3. This setup provided a convenient way to save original records on PC2's disks before freeing the space needed the next day on PC1 for the collection of data. Doing so, at least two copies (CDs + HDs) existed before erasing original files.

Data collected by PC2 via the serial lines server were duplicated on PC3 every day. The whole 4-day survey holds on a single CD. Several copies have been edited.

File formats of all data collected by PC1 and PC2 are given in Annex 2 and 3, respectively. The complete set is archived on about 170 CDs. This large amount of disks is not very convenient for distributing data to partners.

Actually, beam data formed in-line were mostly used during acquisition for display and checking. LMP post-processed the raw transducers data in order to build a better set of beamformed data, by taking into account accurate calibration parameters. The main step of the process are summarized here :

- Removal of residual offsets found in the real and imaginary parts of the raw transducer data
- Amplitude correction based on statistics of the signals received by each transducer during the whole survey
- Phase correction based on a thorough calibration performed in tank
- Removal of the Time Varying Gain applied in line
- Pulse compression
- Beam-forming with dynamic focusing using the Fresnel approximation
- Introduction of a standard correction to compensate for propagation losses
- Coding of the resulting data
- Search for the first bottom return (depth index)

- Estimate of the maximal useful range, beyond which the Signal to Noise Ratio is thought to be too small.

The coding stage reduces significantly the final size of the created files. The whole survey holds now on about 45 CDs when including the interferometric phases, and less than 20 CDs for the versions that discard this information.

This compression is achieved with a simple scheme : For any given time sample, the maximal energy received by all beams is searched. This value is rounded (in dB) to the closest upper integer, and recorded. This value serves as a reference to code with a single byte (on a log scale) the energy of each beamformed sample. The interferometric phases are recorded with 2 bytes (unit = 1.e-4 rad.).

The new file format is described in Annex 4. Only "`integer`" types are used in order to ease the conversion between platforms (e.g. workstations). In addition, the structure of the files is designed to support additional blocks that could be created at miscellaneous post-processing stages.

First versions of software elaborated by LMP were available during the sea trial to build mosaic images with PC3. In Figure 3.3, the image on right shows the kind of display that was available in-line (single ping), during data acquisition on PC1. The corresponding mosaic is shown on left.

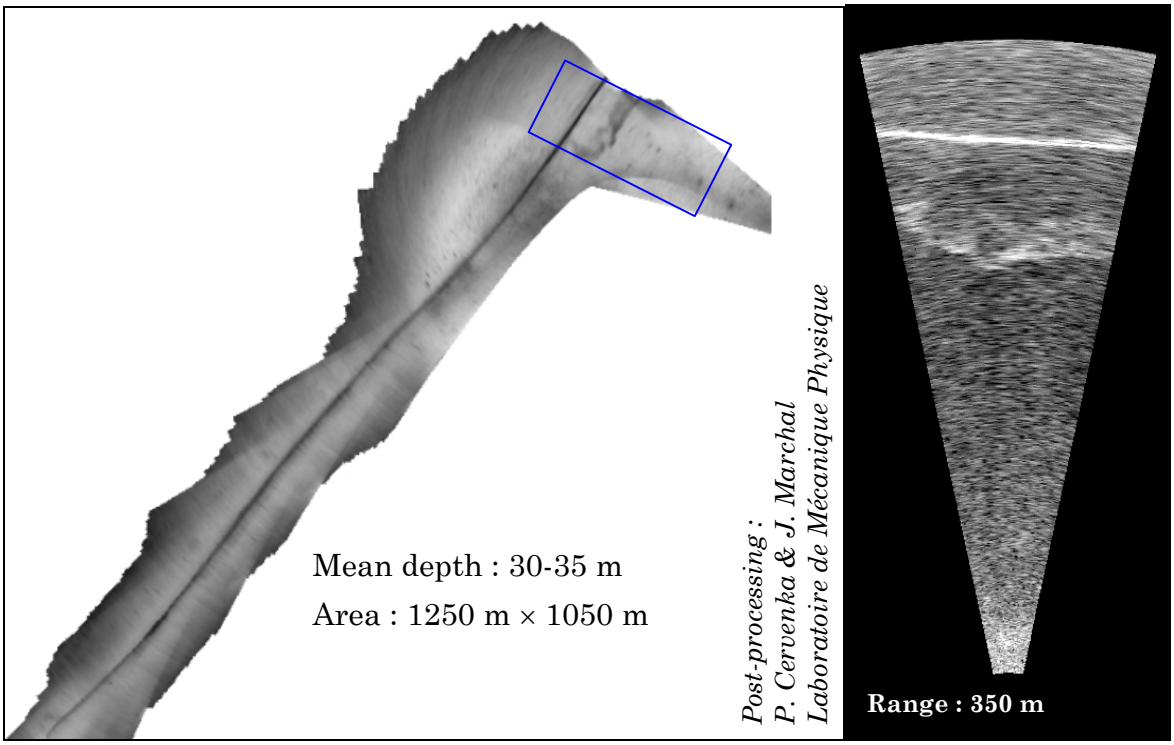

Figure 3.3 : Contact and tracking of a pipeline during the COSMOS survey

3.4 ANNEXES

3.4.1 ANNEX 1 – **PROPRIETARY SONAR BUS**

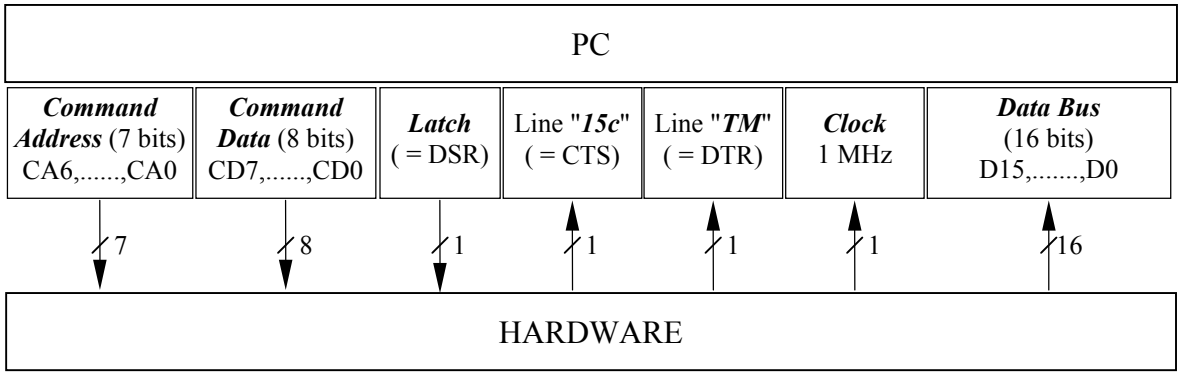

Figure 3.4

COMMANDS BUS

TM enabled :

* ***TM*** line is automatically enabled by HARDWARE as soon as transfer over the DATA BUS is over.
* PC1 can send information through ***Command_Address*** and ***Command_Data*** only while ***TM*** enabled.
* Handshake for the COMMAND BUS is provided with lines ***Latch*** and ***15c*** .

Line ***15c*** is always disabled when ***TM*** is disabled.
As long as PC1 does not send data to HARDWARE, ***Latch*** must be kept disabled.
PC1 is allowed to start sending a data through COMMAND BUS only when ***15c*** is enabled.

15c is first enabled at the same time as ***TM***.

When PC1 is authorized to send data to HARDWARE (***15c*** enabled),
transfer of data that are loaded on lines ***Command_Address, Command_Data*** is initialized when ***Latch*** is enabled.

Enabling ***Latch*** induces a response from HARDWARE : ***15c***.is disabled.

However, because ***15c*** is built with an internal clock (1 MHz),
a random delay that cannot last more than 1µs may occur before ***15c*** is disabled :
Latch must remain enabled at least 1µs to assert properly the request to send.

PC1 must then hold data lines "***Command_Address, Command_Data"***
until ***15c*** is enabled again (= after 15µs delay) :

HARDWARE acknowledges that reception is complete.
Another cycle of data transfer from PC to Hardware can occur.

Finally, ***15c*** is disabled together with ***TM***. and PC1 cannot send data any longer (it is time for PC1 to collect data from DATA BUS).

TM disabled :

* In *External ping synchro* mode (see *Static orders* next), Hardware disables ***TM*** as soon as next ping is trigged (i.e. when ***Command_Address*** = 0X7F is latched)

* In *Internal ping synchro* mode (see *Static orders* next), Hardware disables ***TM*** after a delay of 65536 µs that do not depends on the choice of range.

Command_Address :

* **0X00** Static orders
  Command_Data CD0 - CD1 : Transmit mode (Test, Pulse, Chirp)
  CD2 : Ping synchro mode (internal or external)
  CD3 - CD4 : Max range (4 choices)
  CD5 - CD6 : Transmit level (4 choices)
  CD7 : Choice of taper function

* **0X01 to 0X7E** : Load TVG levels
  Command_Data CD0 to CD6 used (128 levels corresponding to scale 0 - 80 dB).

* **0X7F** : Trigger for next ping if *External ping synchro* mode is selected
  Command_Data irrelevant - hold far range TVG value, but is actually not used.

Note : But for Trigger of next ping in *External ping synchro* mode, previously loaded values apply.

The following table gives several parameters that depends on the chosen modes :

Range (CD5-6)	0	1	2	3
TM disabled (µs)	303104	458752	671744	983040
Samples / channel	1184	1792	2624	3840
Approx. Range (m)	227	344	504	737
Ping rate (µs) (internal trigger)	368640	524288	737280	1048576

With the *Internal ping synchro* mode (hardware), the delay of latency between the end of data transmission and the beginning of next ping is 65536 µs, whatever the chosen range is. With the *External ping synchro* mode (software), there is no minimal delay of latency. During this delay, the PC1 based monitoring unit can send orders and parameters to the sonar unit (mode, range TVG, …).

DATA BUS

Timing

Data rate : One 16bits-word per µs.

⇒ One second of echo recording means about 2Mbytes to collect and store.

Clock pulses last 250ns, occurring at the third quarter of the 1µs time interval during which data to be collected are loaded on DATA BUS. Hence, data are insured to be valid on this bus during the whole clock pulse interval.

Data Structure

Time samples (named here "tixels") concern a period lasting 256 µs, each tixel contains 256 words that are multiplexed at 1 MHz.

One word is an integer number, signed (*signed short*) or not (*unsigned short*); A complex number is represented with 2 words (i.e. 2 *signed short*s).

Tixel format

Number of words	Logical content	Information
128	64 complexes	Transducer data $x_T^{(b)} + jy_T^{(b)}$
124	62 complexes	Preformed beams $x_F^{(b)} + jy_F^{(b)}$
1	1 unsigned integer	PEAK DETECTION $\mathbf{max}\left(\left\|x_T^{(b)}\right\|,\left\|y_T^{(b)}\right\|\right)$ of several tixels, (log scale) planed to ease the elaboration of the TVG correction
1	1 signed integer	Attitude data, multiplexed over 8 tixels (unused ⇒ NULL)
1	1 unsigned integer	TIXEL ADDRESS (12 bits to address 1s)
1	NULL	For multiplex checking purpose

Multiplexing rule for each Tixel (256 values)

$$x_T^{(b)} = \mathrm{A}\left[64(T \bmod 4) + 4(T \div 4) + 2b\right] = \mathrm{A}\left[63(T \bmod 4) + T + 2b\right]$$

$$y_T^{(b)} = \mathrm{A}\left[64(T \bmod 4) + 4(T \div 4) + 2b + 32\right] = \mathrm{A}\left[63(T \bmod 4) + T + 2b + 32\right]$$

with $b = 0, 1$ and $T = 0, \ldots, 31$

$$X_F^{(b)} = \mathrm{A}\left[8F + 2b + 1\right]$$

$$Y_F^{(b)} = \mathrm{A}\left[8F + 2b + 5\right] \text{ with } b = 0,1 \text{ et } F = 1,\ldots,31$$

PEAK_DETECTION(8MSB) = A[1] $\left(\equiv X_0^{(0)}\right)$ and ATTITUDE = A[3] $\left(\equiv X_0^{(1)}\right)$
NULL = A[5] $\left(\equiv Y_0^{(0)}\right)$ and TIXEL_ADDRESS = A[7] $\left(\equiv Y_0^{(1)}\right)$

The following table gives the complete explicit multiplexing order :

	Array 0*(b=0)*				**Array 1***(b=1)*			
	Transd.		**Beam**		**Transd.**		**Beam**	
T or **F**	**x_T**	**y_T**	**X_F**	**Y_F**	**x_T**	**y_T**	**X_F**	**Y_F**
0	0	32	1	5	2	34	3	7
1	64	96	9	13	66	98	11	15
2	128	160	17	21	130	162	19	23
3	192	224	25	29	194	226	27	31
4	4	36	33	37	6	38	35	39
5	68	100	41	45	70	102	43	47
6	132	164	49	53	134	166	51	55
7	196	228	57	61	198	230	59	63
8	8	40	65	69	10	42	67	71
9	72	104	73	77	74	106	75	79
10	136	168	81	85	138	170	83	87
11	200	232	89	93	202	234	91	95
12	12	44	97	101	14	46	99	103
13	76	108	105	109	78	110	107	111
14	140	172	113	117	142	174	115	119
15	204	236	121	125	206	238	123	127
16	16	48	129	133	18	50	131	135
17	80	112	137	141	82	114	139	143
18	144	176	145	149	146	178	147	151
19	208	240	153	157	210	242	155	159
20	20	52	161	165	22	54	163	167
21	84	116	169	173	86	118	171	175
22	148	180	177	181	150	182	179	183
23	212	244	185	189	214	246	187	191
24	24	56	193	197	26	58	195	199
25	88	120	201	205	90	122	203	207
26	152	184	209	213	154	186	211	215
27	216	248	217	221	218	250	219	223
28	28	60	225	229	30	62	227	231
29	92	124	233	237	94	126	235	239
30	156	188	241	245	158	190	243	247
31	220	252	249	253	222	254	251	255

3.4.2 ANNEX 2 – FORMAT OF THE RECORDED ACOUSTIC DATA FILES

Raw files recorded by PC1 contains :

- A file header (structure "`def_cosmos_rawfile_hdr`" , see below)
- a sequence of records, one record per ping.

The size of each file is limited to about 30 MB. Each ping is identified by a unique string that is build with the local time of ping trigger, counted is seconds since the 1st January 1970, e.g. "940929259_27" where "940929259" is the number of seconds and "27" a fractional complement in centiseconds. The file name is the identifier of the first ping that it contains, with the suffix "raw".

Each record is made of two components :

- a record header (structure "*`def_cosmos_record_hdr`*", see below)
- an array of **`short`**s whose size (`nb_data`) is specified in the record header.

The array contains a multiple of 256 words. Each set of 256 words carries information about one time sample (a "tixel"), that corresponds to a receiving period lasting 256 µs. The multiplexing rule is explicited in Annex 1.

```
typedef struct {
  long  time;           // number of seconds elapsed since 1th January 1970
  short millitm;
  short timezone;
  short dstflag;
} def_timeb;            // mimics stucture used in ftime() (WIN32 function)

typedef struct {
  char      comment[256];
  def_timeb init_time;        // time at acquisition program start
} def_cosmos_rawfile_hdr;

typedef struct {
  unsigned short state;      // describes mode of operation
  short          nb_tixels;  // theoretical number of pixels to be received
  short          tvg[127];   // Tvg interval = 32 tixels = 6.14 m
} def_cosmos_setting;

typedef struct {
  long      relative_ping_time; // in ms, relative to starting cosmos_surv
  def_timeb ping_time;          // given by ftime at ping start
  char      time_string[64];    // sssssssss_cc    (cc : centiseconds)
  long      ping_number;        // starting from 0, at beginning of process
  long      nb_data;            // 256L * nb_tixels, or zero
  int       error_code;
} def_cosmos_infos;


typedef struct {
  def_cosmos_setting setting;
  def_cosmos_infos   infos;
} def_cosmos_record_hdr;
```

3.4.3 ANNEX 3 – FORMAT OF ATTITUDE AND NAVIGATION FILES

GPS (latitude and longitude), heading, attitude (roll, pitch, heave), ping synchronization, time and date are recorded in *.ser files by PC2. These files are made of contiguous sequences of structures ("XTFPACKETHEADER", "XXX_SER"), where the first structure "XTFPACKETHEADER" permits to identify the nature of the following "XXX_SER" structure.

The following pieces of C code is derived from TEISA software. It gives all the needed information to read and process such files. The only members written in **bold** face are actually used. Timetags corresponding to the **same** type of packets are ordered in the file. It **does not** guaranty that all Timetags are ordered. See also the important notice at the end of this Annex.

```
#define Sync_tag_delay 32L // ms
#define Gps_tag_delay  58L // ms
#define Head_tag_delay 37L // ms


// Type of data
//       (Values given to member HeaderType of struct XTFPACKETHEADER)
typedef enum {
  GPS_DATA  = 0,          // GPS info (longitude and latitude)
  HDSP_DATA = 1,          // Heading Info
  ATT_DATA  = 2,          // Heave, roll, pitch infos
  TIME_DATA = (BYTE)0XFF,
  SYNC_DATA = (BYTE)0XFE, // COSMOS synchro
} TypeOfData;


// UTC Time and UTC date structures
typedef struct {
  char  hh;
  char  mn;
  float ss;
} UTC_Time;


typedef struct {
  char  dd;
  char  mm;
  short yy;
} UTC_Date;


// Packet header (needed to identify the following structure)
typedef struct {
   WORD  MagicNumber;        // Always set to 0xFACE
   BYTE  HeaderType;         // set to a value given in enum TypeOfData
   BYTE  SubChannelNumber;
   WORD  NumChansToFollow;
   WORD  Reserved1[2];
   DWORD NumBytesThisRecord; // Total byte count, including this header
} XTFPACKETHEADER;
```

```
//
//                      GPS structure
//
typedef struct {

  DWORD    UP;         // update flag (test it as VL)
  DWORD    VL;         // if(VL & (1L << 2)) X and Y are valid
  DWORD    TimeTag;    // in milliseconds, PC2 clock
  UTC_Time TimeUTC;
  UTC_Date DateUTC;
  double   X;          // Longitude (decimal degrees, > E, < W)
  double   Y;          // Latitude (decimal degrees)
                       // Actually, X and Y are quantized at 1/1000th minute
  short    U;
  short    GPS_Quality;
  short    NumSatUsed;
  float    HDOP;
  float    Altitude_MSL;
  float    Geoidal_Separation;
  float    AgeOfDGPS;
  short    DGPS_ID;
  float    Convergence;
  char     GPS_Mode;
  long     Fixnumber;
  char     Reserved1[43];

} GPS_SER;

//
//                      HDSP packet structure (heading)
//
typedef struct {

  DWORD UP;
  DWORD VL;                // if(VL & (1L << 2)) TrueHeading is valid
  DWORD TimeTag;           // in milliseconds, PC2 clock
  float SensorHeading;
  float MagneticHeading;
  float TrueHeading;       // Heading from Geographical North
  float MagneticDeviation;
  float MagneticVariation;
  float COG_True;
  float COG_Magnetic;
  float SOG;
  char  Position_Mode_Indicator;
  char  Reserved1[5];

} HDSP_SER;

//
//                      ATT packet structure (Attitude)
//
typedef struct {

  DWORD    UP;
  DWORD    VL;
  float    GDOP;
  int      SystemType;
  float    Pitch;       // in degrees
  float    Roll;        // in degrees
  float    Heave;       // in degrees
  float    Yaw;
  DWORD    TimeTag;     // in milliseconds, PC2 clock
  float    TrueHeading;
  UTC_Time TimeUTC;
  UTC_Date DateUTC;
  short    NumSatAbove;
  short    NumSatInitial;
  float    RMS_Solution;
  char Reserved[56];

} ATT_SER;
```

```
//
//                      Time and date packet structure
//
typedef struct {

  DWORD    UP;
  DWORD    VL;
  WORD     TimeTag;     // in milliseconds, PC2 clock
  UTC_Time TimeUTC;     // if(VL & 1L)         TimeUTC is valid
  UTC_Date DateUTC;     // if(VL & (1L << 1)) DateUTC is valid
  WORD     Reserved[14];

} TIME_SER;


//
//                      (Ping) Synchro packet structure
//
typedef struct {

  DWORD UP;
  DWORD VL;
  DWORD TimeTag;        // in milliseconds, PC2 clock
  BYTE  message[38];    // Ping identifier send by the COSMOS PC

} SYNC_SER;
```

Important notice

Corrections must be performed to get the proper "Timetag" of the "Message" carried by several structures : **Sync**, **Heading** and **GPS** data are shifted, i.e. the correct "Timetag" to apply to "Message" contained in the packet is the "Timetag" contained in the next packet (of the same type), with an additional small delay. Let's consider for example a sequence of packets of the same type, as recorded :

Timetag_i-1	Message_i-1
Timetag_i	Message_i
Timetag_i+1	Message_i+1

Actually, the proper association is the following :

…	
(Timetag_i - delay)	Message_i-1
(Timetag_i+1 - delay)	Message_i
…	

The value of "delay" is given (in ms) by :

Sync_tag_delay	= 32 for Sync packets,
Gps_tag_delay	= 58 for GPS packets,
Head_tag_delay	= 37 for Heading packets

For Sync packets, "Message" is the ping identifier string sent by PC1 (LMP) to the PC2 (TEISA) ;

For GPS packets, "Message" is latitude and longitude ;

For Heading packets, "Message" is the true heading.

3.4.4 ANNEX 4 – **FORMAT OF POST-PROCESSED DATA**

The general organization of the post-processed data files is described below :

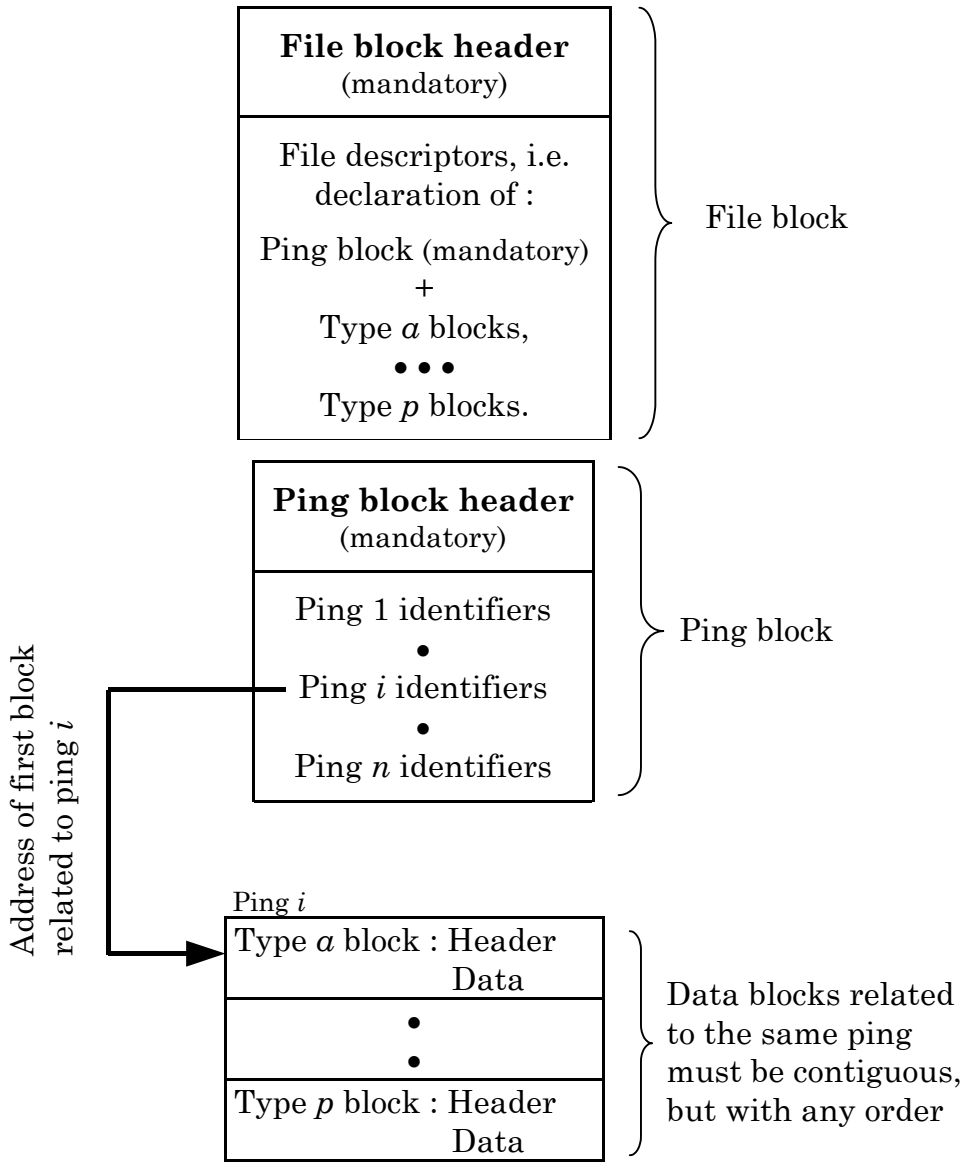

Figure 3.5

Files are built with contiguous blocks. A file must include a unique "File block" and a unique "Ping block". The "File block" describes the kind of data that the file contains. The "Ping block" is a table that lists miscellaneous references to each ping (Time stamp, identifier, address within the file of the other blocks related to the ping…). The bulk of the file content consists of the other blocks which may concern : Backscattered levels, interferometric phases, positions, bathymetric information, etc…

The following headers give the needed structures (in C code) for files that have been distributed to DIBE and IFREMER.

```
typedef enum {
  Flhd_pk = 0, // File header packet
  Pgid_pk = 1, // Ping identification packet
  Acou_pk = 3,
  Phas_pk = 4,
} typeofpacket;


typedef enum {
  Leg_begin_stb = 0,
  Leg_end_stb   = 1,
  Base_0_stb    = 2,
  Base_1_stb    = 3,
} status_bit;


typedef struct {
  long sizeofpacket;
  long typeofpacket;
} def_packet_id;


typedef struct {
  short yy;
  char  mm;
  char  dd;
  char  hh;
  char  mn;
  char  ss;
  short millis;
} def_time_stamp;


typedef struct {
  def_packet_id packet_id; // typeofpacket = Flhd_pk
                           // sizeofpacket = sizeof(def_file_hd) +
                           //                nb_file_id*sizeof(def_file_id)
  char  string[256];
  long  nb_file_id;
} def_file_hd;


typedef long def_file_id;


typedef struct {
  def_packet_id packet_id; // typeofpacket = Pgid_pk
                           // sizeofpacket = sizeof(def_ping_hd) +
                           //                nb_ping_id*sizeof(def_ping_id)
  long nb_ping_id;
} def_ping_hd;
```

```
typedef struct {
  def_time_stamp time_stamp;
  char  time_string[16];   // ssssssssss_cc    (cc : centiseconds)
  long  timetag;
  long  index;
  long  address;          // point to beginning of 1st block for that ping
} def_ping_id;


typedef struct {
  def_packet_id packet_id; // typeofpacket = Acou_pk
                           // sizeofpacket = sizeof(def_acou_hd) +
                           //              depends on number of bases, i.e.
                           //   (0 or 1 ) * acou_hd.nb_tixels*sizeof(char)
                           // + (0 or 1 or 2) * sizeof(char) *
                           //             acou_hd.nb_beams*acou_hd.nb_tixels
                           // + (0 or 1) * sizeof(short) *
                           //             acou_hd.nb_beams*acou_hd.nb_tixels
  long  status;            // if (status & (1L<<base_0_stb)) -> base_0,
                           // if (status & (1L<<base_1_stb)) -> base_1
  short nb_beams;
  short nb_tixels;
  short aperture;          // 1/100 deg.
  short noise_threshold;   // dB  default=-32000 (undefined)
  short noise_index;       // default : nb_tixels
  short depth_threshold;   // dB  default=-32000 (undefined)
  short depth_index;       // default : 0
                           // (if < 0, abs(depth_index) is questionable)
  short source_level;      // in 0.1 dB rms ref. 1µPa @ 1m
  short sensibility;       // in 0.1 dB (system_unit / µPa)
  short dynamic;           // dB
} def_acou_hd;


typedef struct {
  def_packet_id packet_id; // typeofpacket = Phas_pk
                           // sizeofpacket = sizeof(def_phas_hd) +
                           //         sizeof(short) *
                           //        angle_hd.nb_beams * angle_hd.nb_tixels
  long  status;
  short nb_beams;
  short nb_tixels;
} def_phas_hd;
```

```
/* Examples of blocks :

File_block : def_file_hd  file_hd;
             def_file_id  file_id[file_hd.nb_file_id];  // typeofpacket

Ping_block : def_ping_hd  ping_hd;
             def_ping_id  ping_id[ping_hd.nb_ping_id];

Acou_block : def_acou_hd  acou_hd;
             short        max_level[acou_hd.nb_tixels]; // in dB
  //if(ac_hd.status&(1L<<Base_0_stb))
           unsigned char beams_base0[acou_hd.nb_beams][acou_hd.nb_tixels];
  //if(ac_hd.status&(1L<<Base_1_stb))
           unsigned char beams_base1[acou_hd.nb_beams][acou_hd.nb_tixels];

Phas_block : def_phas_hd phas_hd;
             short        phase[phas_hd.nb_beams][phas_hd.nb_tixels];
                                                          // 1e-4*rad.
```

Examples of files :

Structure of Acu files

File_block + Ping_block + (ping_hd.nb_ping_id) Acou_block

Structure of Acp files

File_block + Ping_block + (ping_hd.nb_ping_id) (Acou_block + Phas_block)